



Standard Model and Beyond

21-23 October 2022
Katowice
Europe/Warsaw timezone

Probing strong interactions with ALICE

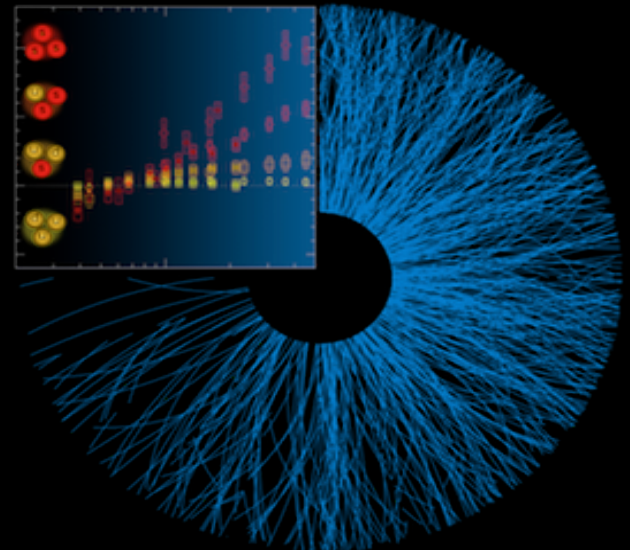
Jacek Otwinowski (IFJ PAN)

On behalf of the ALICE Collaboration
Katowice, 21 Oct 2022



OUTLINE

- ALICE experiment
- Hyperon interactions
- Quarkonium production
- Dead-cone measurement
- Summary and Outlook

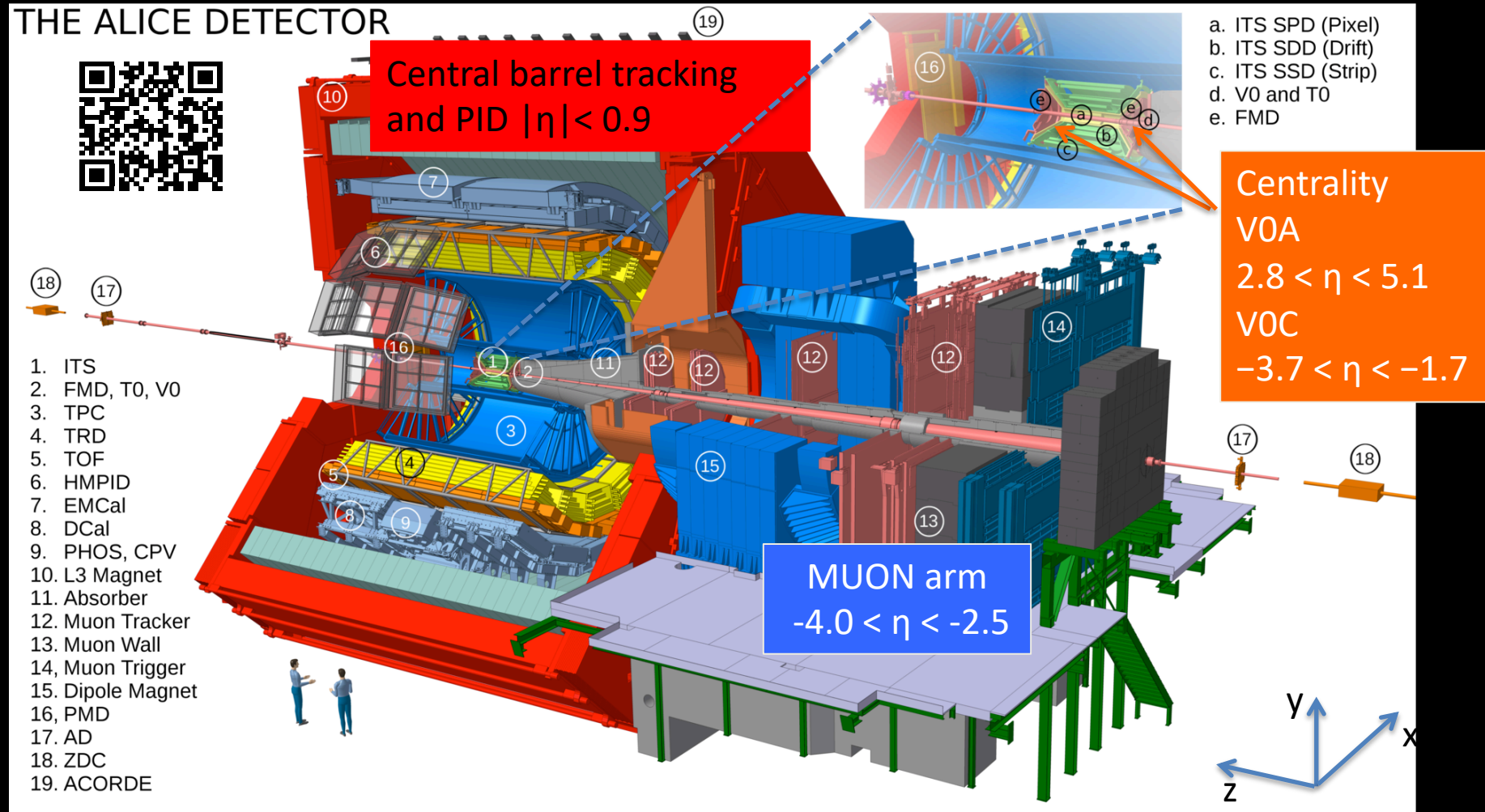


A Large Ion Collider Experiment



- Excellent particle identification capabilities over a wide p_T range 0.1-20 GeV/c
- Good momentum resolution $\sim 1\text{-}5\%$ for $p_T = 0.1\text{-}50$ GeV/c

THE ALICE DETECTOR

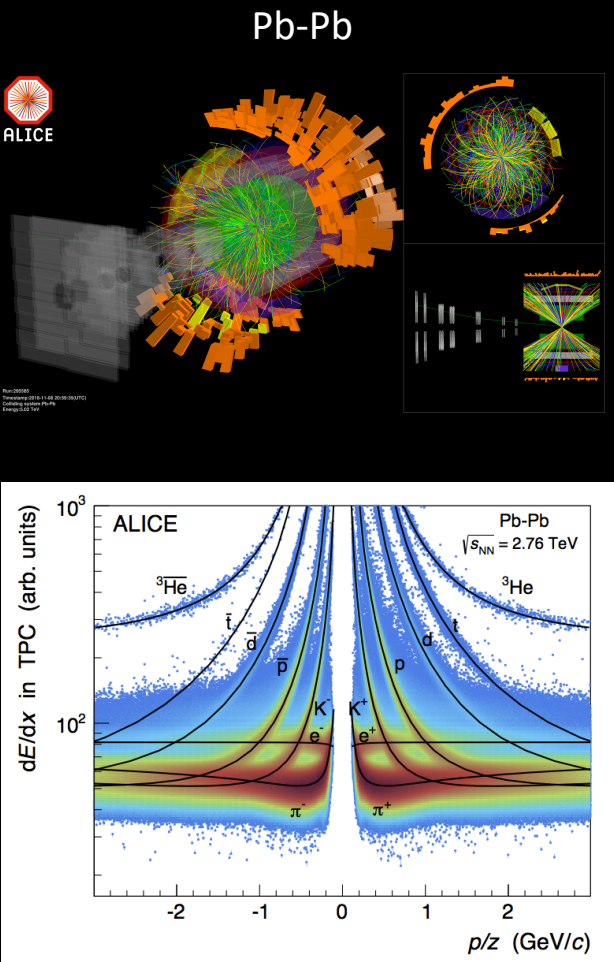


ALICE at work since 2009



System	Year	$\sqrt{s_{NN}}$ (TeV)	L_{int}
Pb-Pb	2010-2011	2.76	$\sim 75 \mu b^{-1}$
	2015	5.02	$\sim 250 \mu b^{-1}$
	2018	5.02	$\sim 0.9 nb^{-1}$
Xe-Xe	2017	5.44	$\sim 0.3 \mu b^{-1}$
p-Pb	2013	5.02	$\sim 15 nb^{-1}$
	2016	5.02, 8.16	$\sim 3 nb^{-1}, \sim 25 nb^{-1}$
pp	2009-2013	0.9, 2.76, 7, 8	$\sim 200 \mu b^{-1}, \sim 100 \mu b^{-1},$ $\sim 1.5 pb^{-1}, \sim 2.5 pb^{-1}$
	2015-2018	5.02, 13	$\sim 1.3 pb^{-1}, \sim 59 pb^{-1}$
	2022-	13.6	Just started

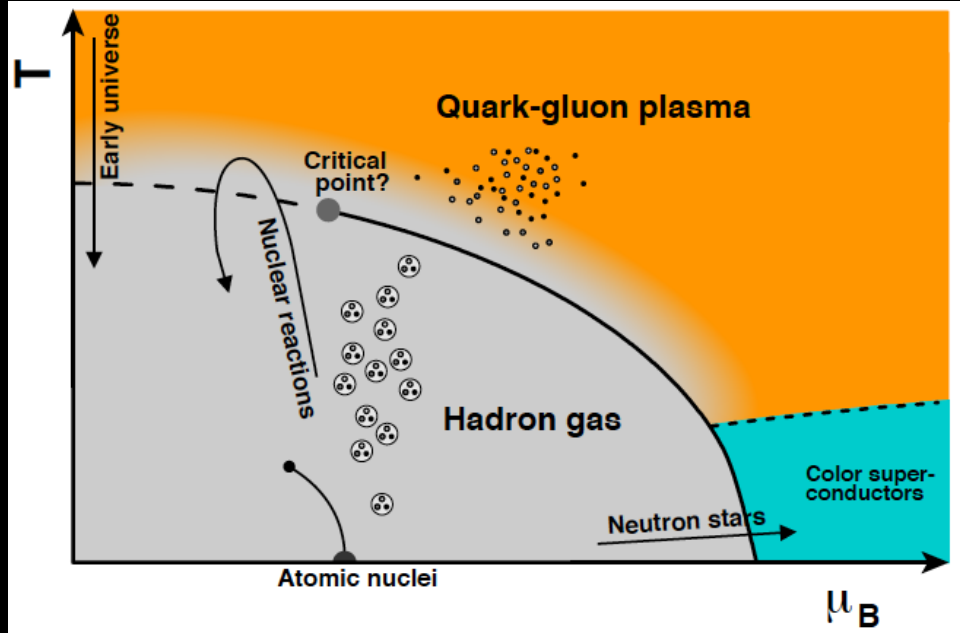
- Energy and system dependence studies of particle production
- Large statistics of pp, p-Pb and Pb-Pb collisions at the same $\sqrt{s_{NN}}$



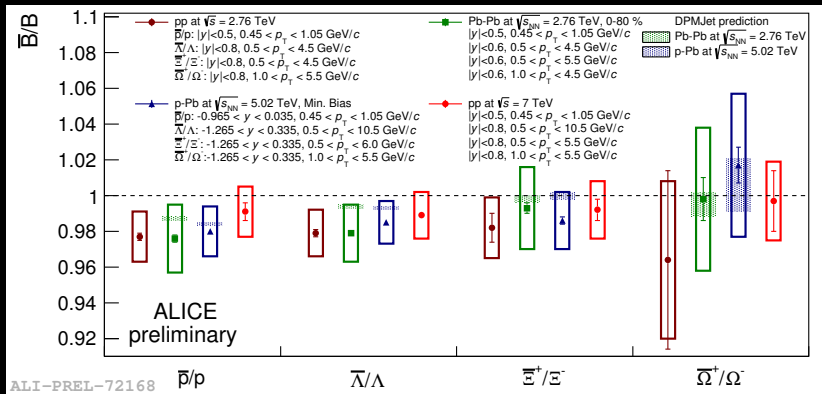
→ Initial and final state effects on particle production

ALICE case

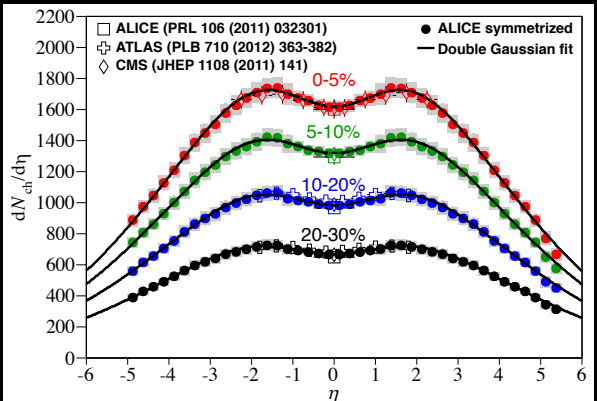
ALICE probes nuclear matter at $\mu_B \sim 0$ and high temperature



Lattice QCD: Hadron gas to quark-gluon plasma
 $(\mu_B = 0, T_C = 156.5 \pm 1.5 \text{ MeV},$
 $\epsilon_C = (0.42 \pm 0.06) \text{ GeV/fm}^3$, smooth crossover)
A. Bazavov et al. Phys. Lett. B 795 (2019) 15



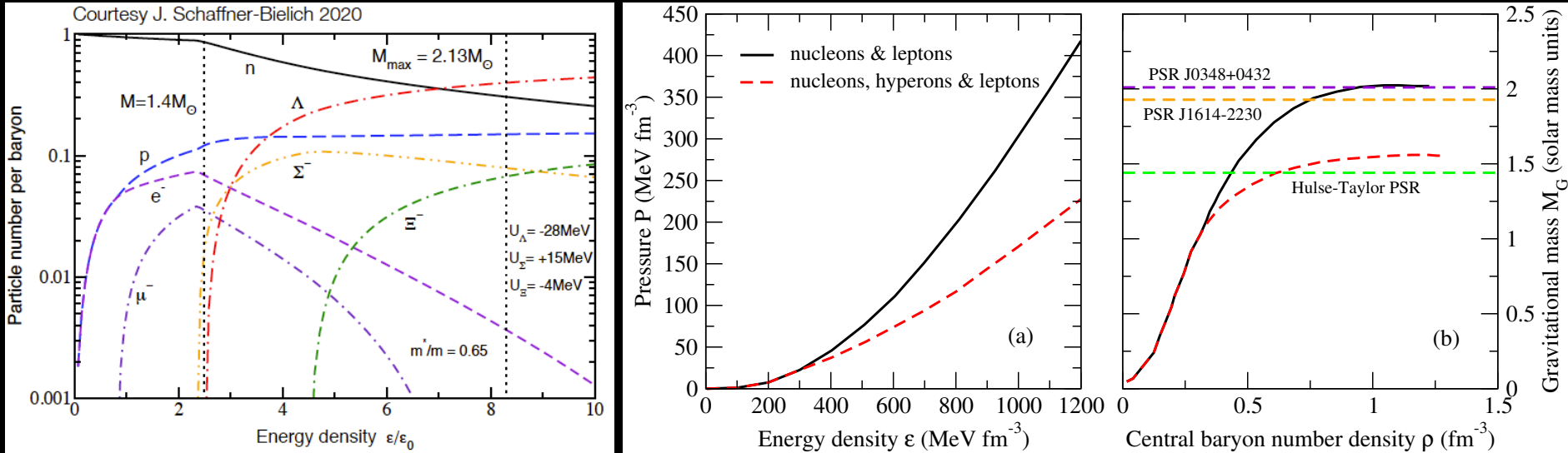
Phys. Lett. B 726 (2013) 610-622



Central Pb-Pb collisions:
 $\varepsilon \sim 14 \text{ GeV/fm}^3 \gg \epsilon_c$

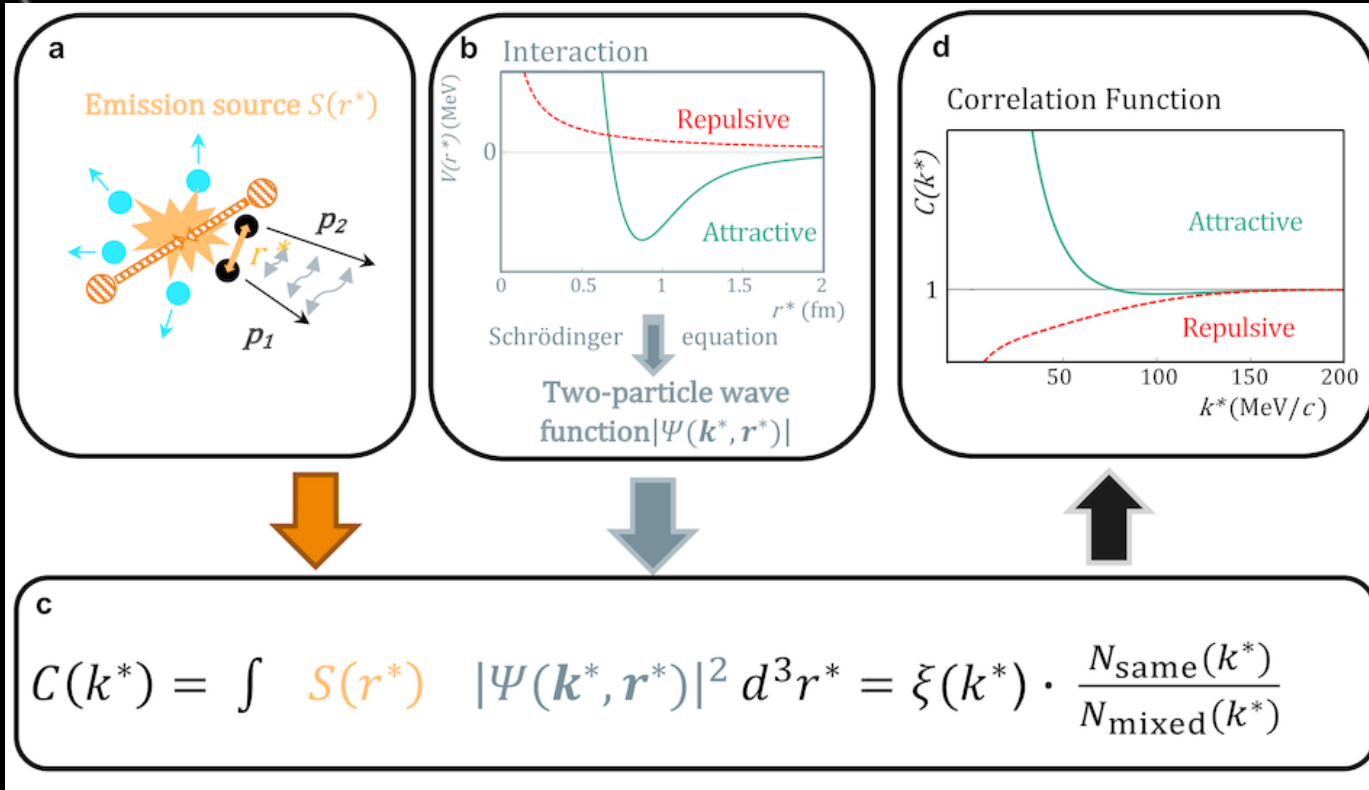
Hyperon “puzzle”

I. Vidaña, Proc. R. Soc. A 474: 20180145



- Hyperons should appear in the inner core of neutron stars at high densities → softening of EoS
- Astrophysical observations of pulsars rule out currently proposed EoS with hyperons
 - Additional repulsion: Y-Y repulsive potential, three-body forces (NNY, NYY, YYY), quark-gluon plasma below the hyperon threshold (hybrid neutron stars)...?
- Small statistics of scattering data for hyperons and hypernuclei → femtoscopy correlations

Femtoscopy correlations to study hadron interactions



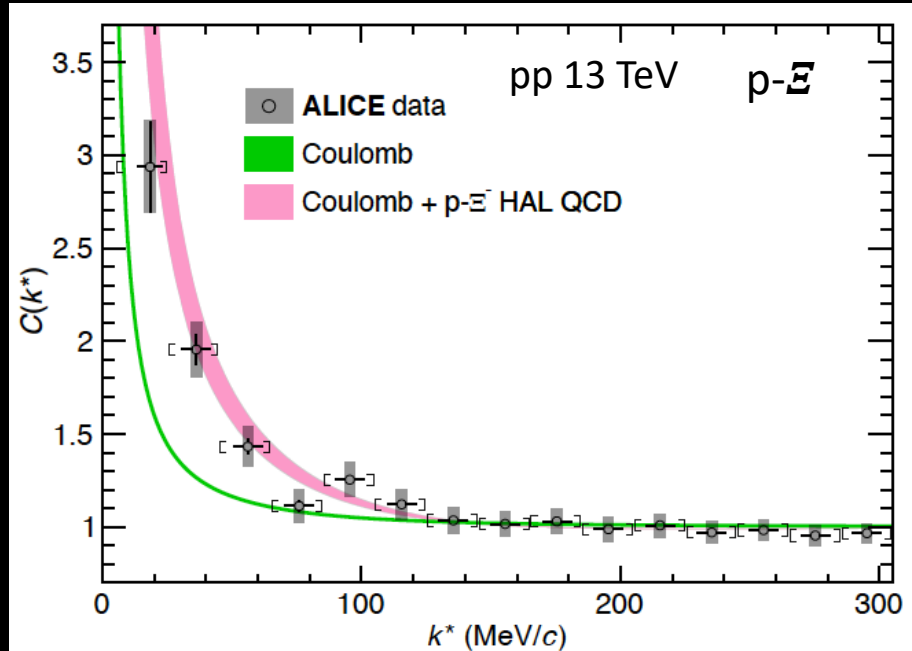
- Origin of correlations: quantum interference, resonances, conservation laws or final-state interactions
- Final-state interactions dominate at small k^*

Today multistrange baryon interactions!

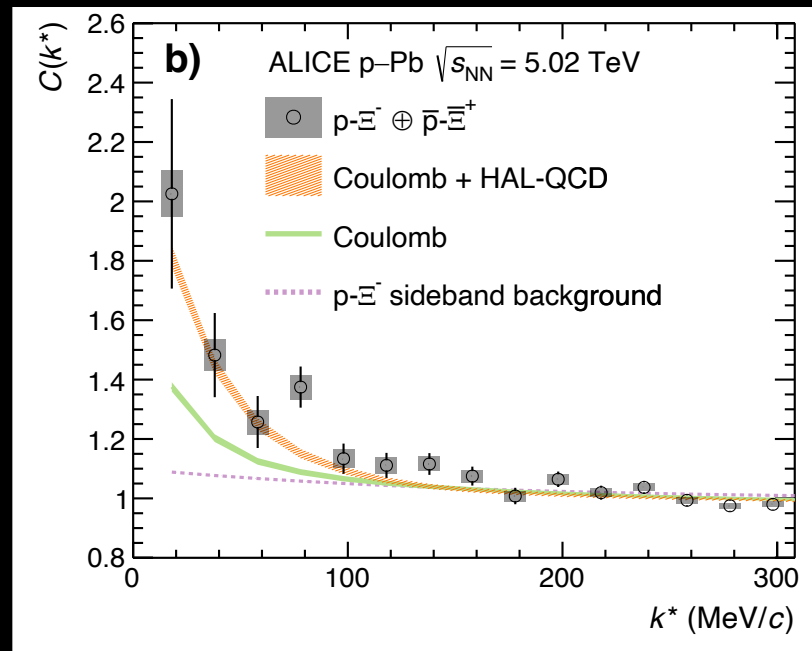
p- E interaction in pp and p-Pb

First measurement of multi-strange baryon interaction

Nature 588, (2020) 232



PRL 123, 112002 (2019)

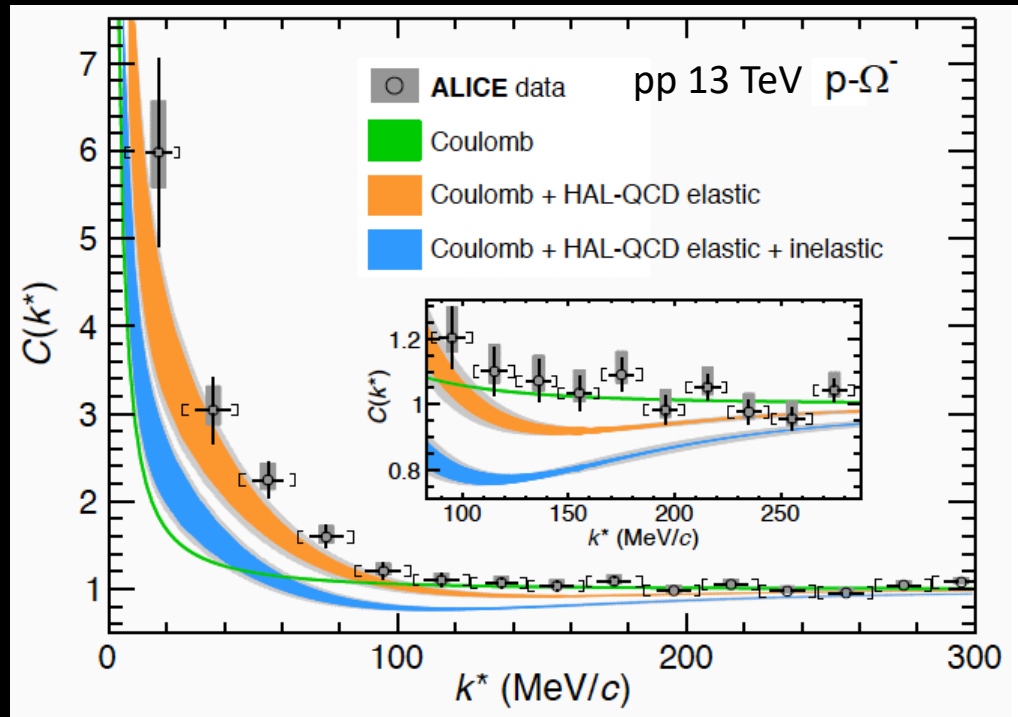


- p- Ξ interaction is attractive HAL QCD: NPA 998 (2020) 121737, PLB 792 (2019) 284
 - No indication of bound state in data
 - p- Ξ interaction stronger than Coulomb → observation of strong interaction
 - Coulomb + HAL QCD in agreement with p- Ξ measurements
 - Inelastic processes p $\Xi \rightarrow \Lambda\Lambda, \Lambda\Sigma, \Sigma\Sigma$ have negligible effect on correlation function

p- Ω interaction in pp

Searching for the p- Ω bound state!

Nature 588, (2020) 232



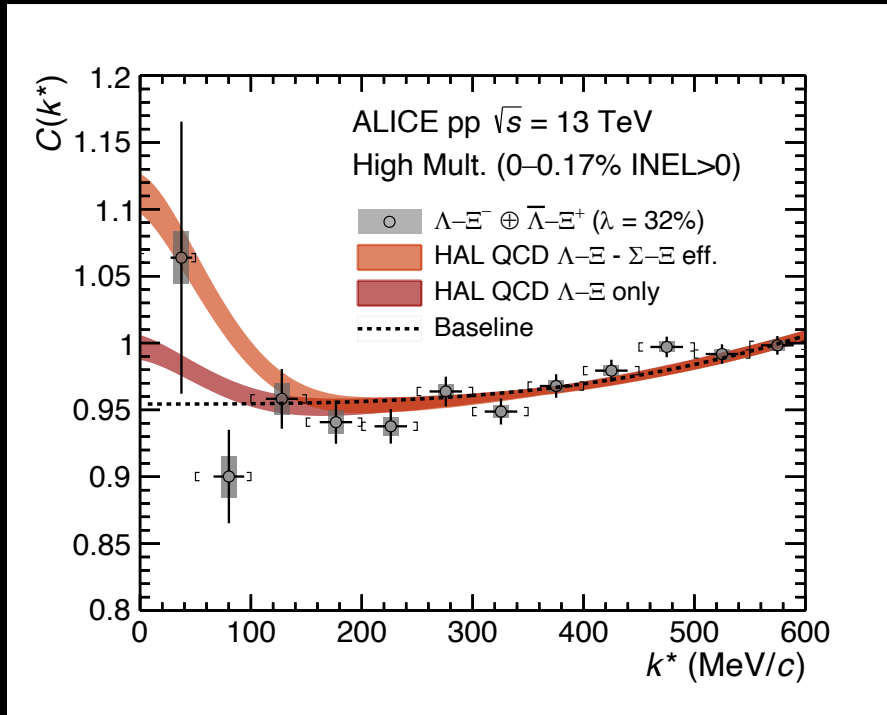
- p- Ω interaction is attractive
 - No indication of bound state in data
 - p- Ω interaction stronger than Coulomb → observation of strong interaction
 - Lattice calculations underestimate measurements (inelastic channels $p\Omega \rightarrow \Lambda\Xi, \Sigma\Xi$ not included yet).
- Two limiting cases:
- Neglecting inelastic channel
 - Inelastic channel completely dominated by strangeness rearrangement
 - Bound state predicted by theory for both cases ($B \sim 2.5$ MeV)

HAL QCD: NPA 998 (2020) 121737, PLB 792 (2019) 284

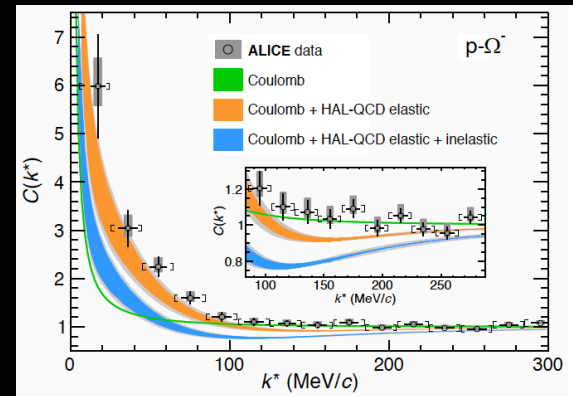
Λ - Ξ interaction in pp

The first measurement of Λ - Ξ interaction

Phys. Lett. B 833 (2022) 137272



- Data supports predictions of very weak Λ - Ξ interaction (baseline denotes no interaction)
- No bound state seen in data
- Influence of coupled channels (Σ - Ξ , N - Ω) on the correlation function requires better statistics



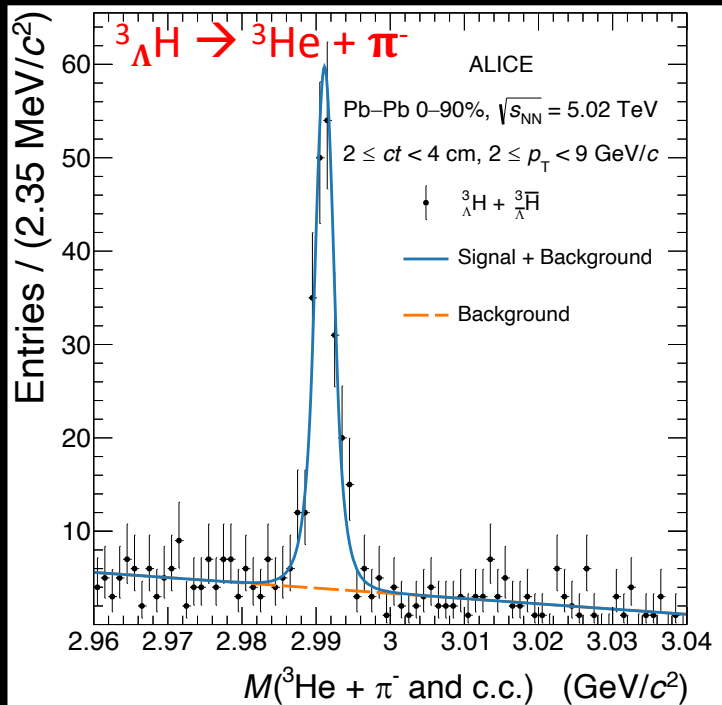
→ More data to set better constraints on p - Ω^- bound state!



(Anti-)hypertriton lifetime



arXiv:2209.07360

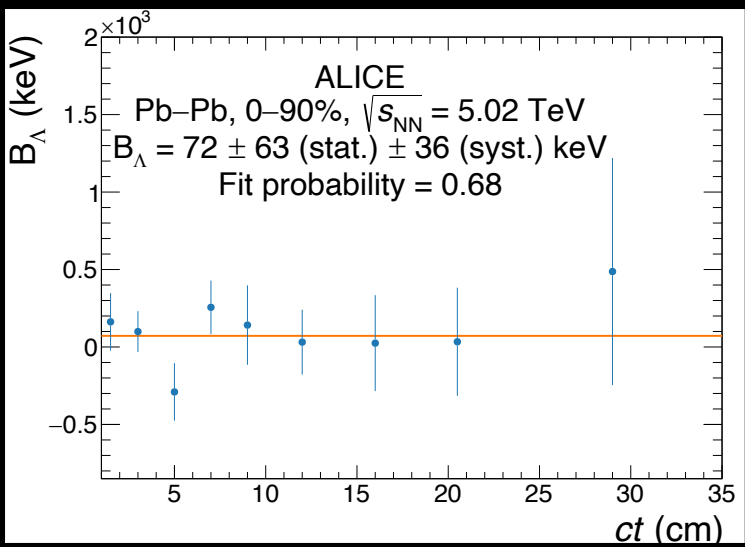
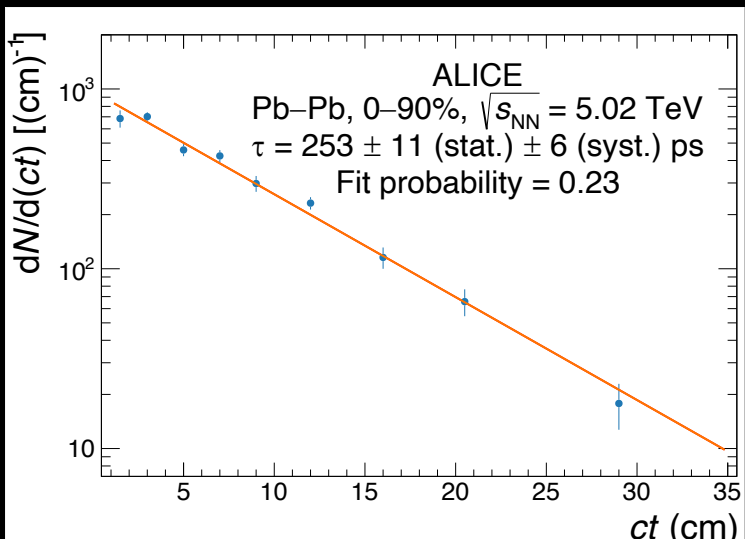


$$c \cdot t = M \cdot L \cdot c/p$$

$$M = 2.99116 \pm 0.00005 \text{ GeV}/c^2$$

L - decay length

p - hypertriton momentum

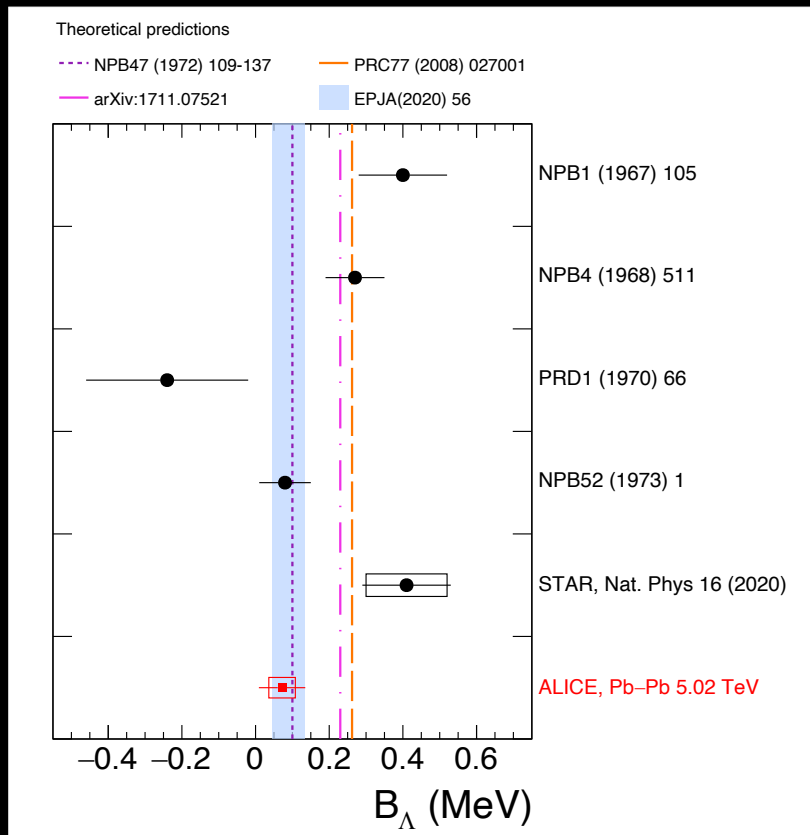
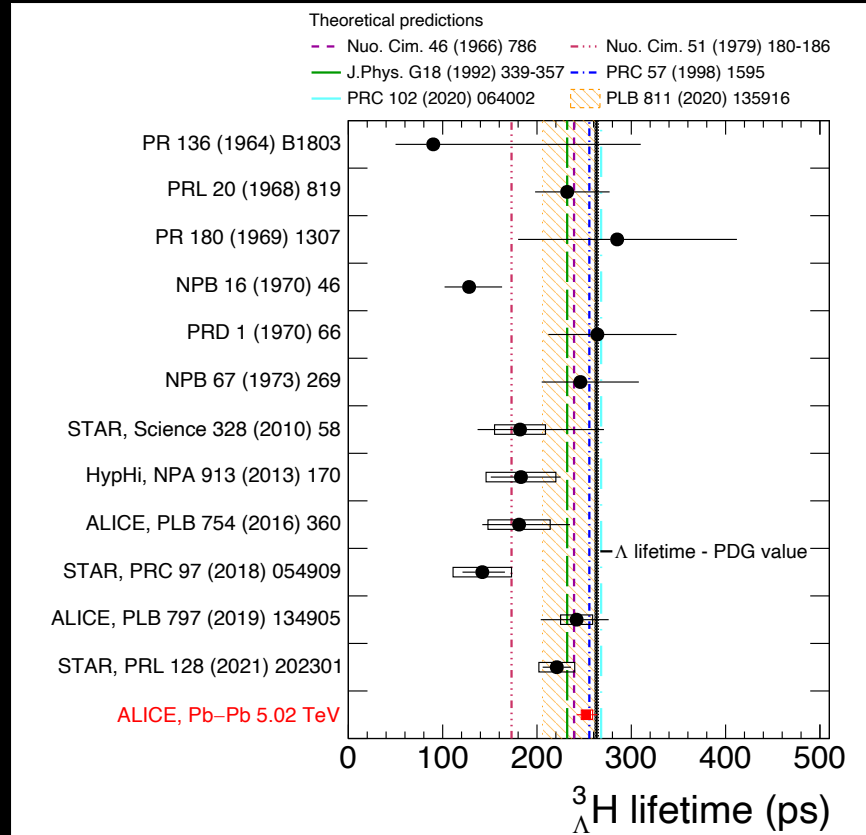


(Anti-)hypertriton lifetime

arXiv:2209.07360

$$\tau = 253 \pm 11(\text{stat.}) \pm 6 (\text{syst.}) \text{ ps}$$

$$B_\Lambda = 72 \pm 63(\text{stat.}) \pm 36 (\text{syst.}) \text{ keV}$$



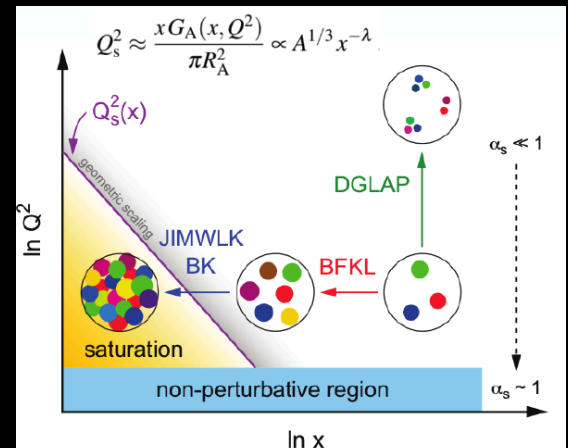
- The most precise (anti-)hypertriton lifetime measurement so far
- (anti-)hypertriton lifetime compatible with that of free Λ
 → Extremely weak interaction of Λ with two other nucleons

Quarkonium production

Quarkonia are excellent probes of initial and final-state effects

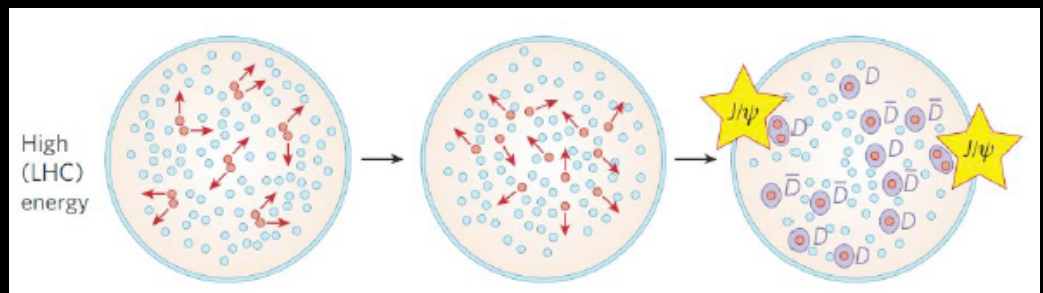
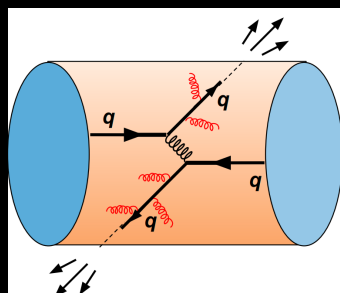
Initial state

- Modification of Parton Distribution Functions
- Gluon saturation and Color-Glass Condensate (CGC)
 E. Iancu et al. Nucl. Phys. A692 (2001) 583



Final state

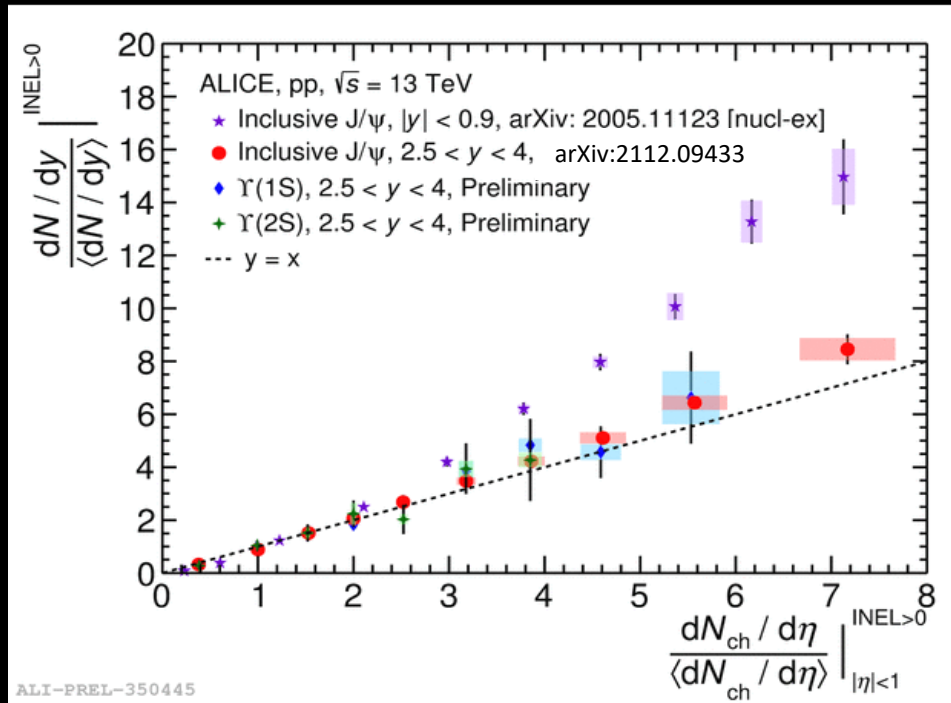
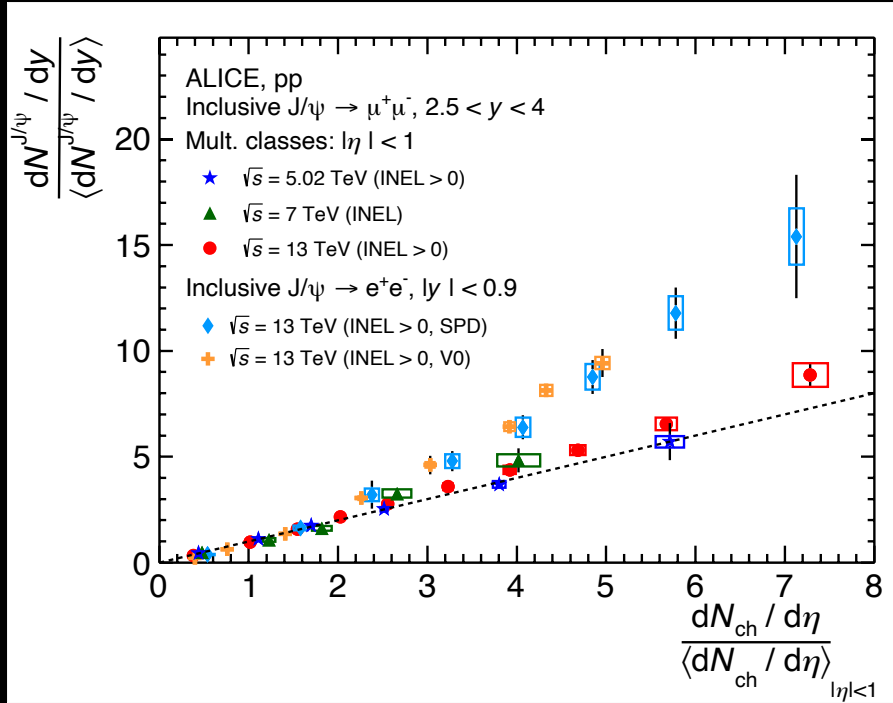
- Parton energy loss in quark-gluon plasma (jet quenching)
- Dissociation of charmonium states in hot medium
 A. Rothkopf Phys. Rept. 858 1, T. Matsui & H. Satz Phys. Lett. B178 (1986) 416
- Recombination of charm and anti-charm quarks
 P. Braun-Munzinger & J Stachel Phys.Lett. B490 (2000) 196
 R Thews et al. Phys. Rev. C 63:054905



Quarkonium production in pp

Testing multi-parton interactions (MPI)

arXiv:2112.09433

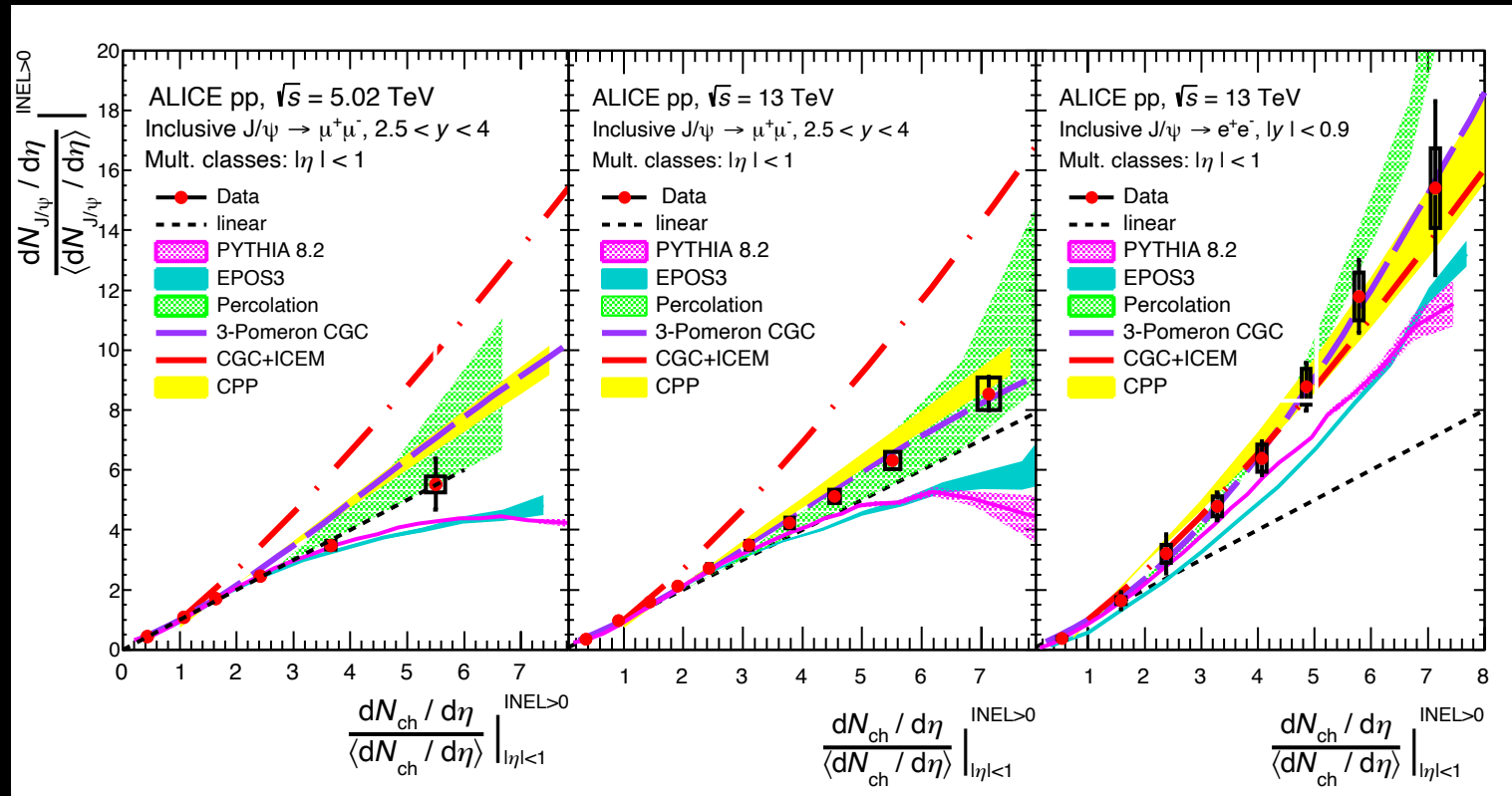


- Linear increase with charged-particle multiplicity at forward rapidity
- Stronger than linear increase with charged-particle multiplicity at central rapidity
- Weak energy dependence

→ More gluons available at central rapidity

J/ ψ production in pp collisions vs models

arXiv:2112.09433



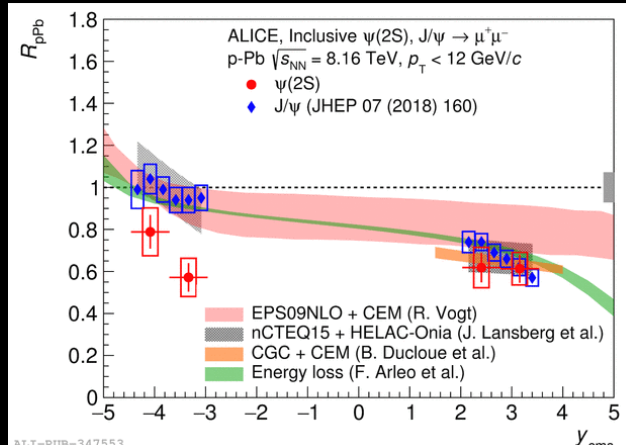
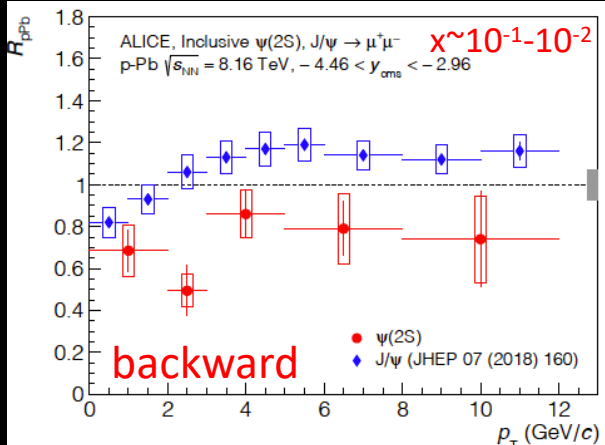
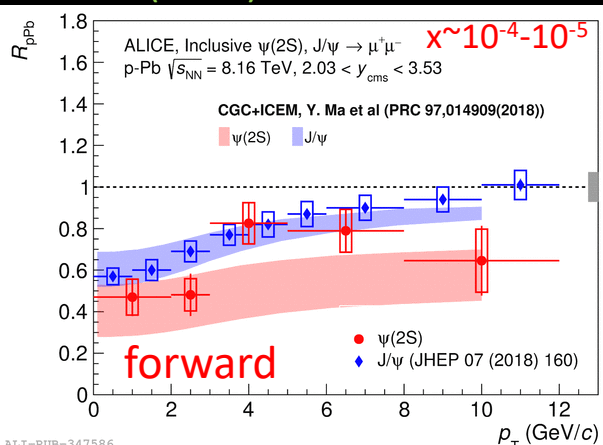
- PYTHIA8 – Lund string-based including color reconnection (CR) (T. Sjöstrand et al.)
- EPOS3 – Gribov-Regge + pQCD, includes non-linear effects, MPI and viscous hydrodynamics (Werner et al.)
- Percolation – color strings exchange between the projectile and target (Ferreiro et al.)
- 3-Pomeron CGC - Color Glass Condensate for initial states including 3 gluon fusion processes (Ryskin et al.)
- CGC + ICM – Color Glass Condensate for initial states+ NRQCD framework for J/ ψ hadronization (Tribedy et al.)
- CPP – pheno. parametrisation of mean J/ ψ and light-flavor multiplicities ($N \sim a N_{\text{coll}}$) (Kopeliovich et al.)

Charmonium production in p-Pb

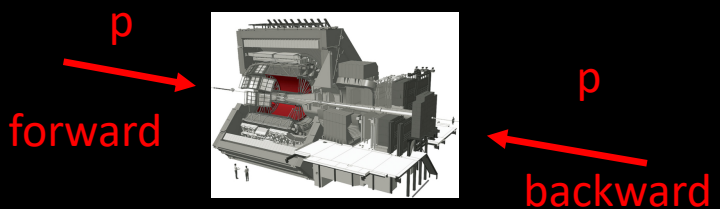
Bjorken-x dependence of charmonium production

JHEP07 (2020) 237

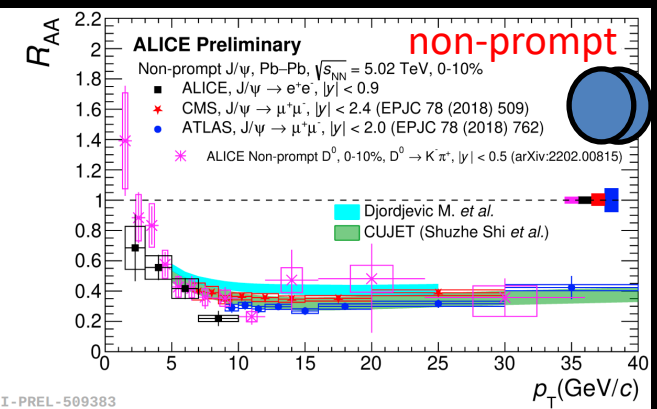
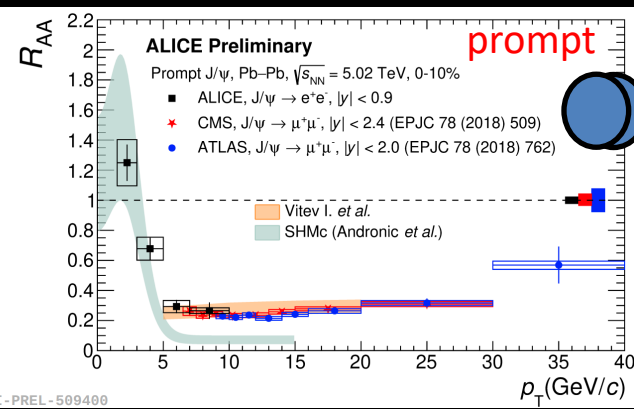
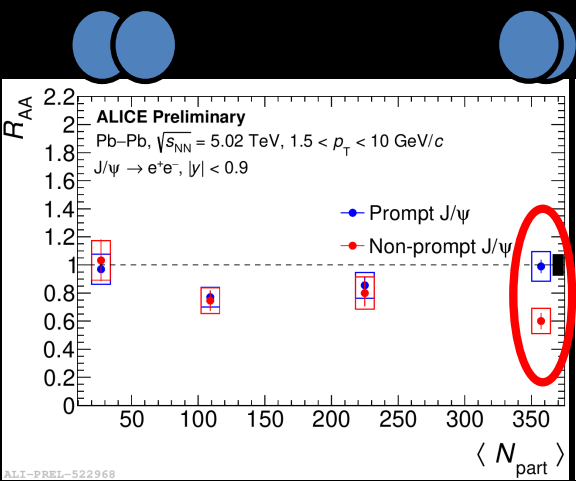
$$R_{pPb} = \frac{d^2\sigma_{pPb}}{dp_T dy} / \frac{d^2\sigma_{pp}}{A dp_T dy}$$



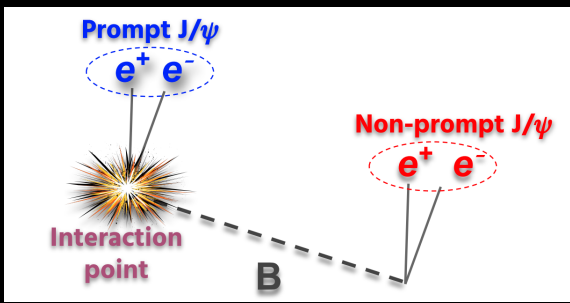
- Measurements for p-Pb (forward rapidity) and Pb-p (backward rapidity) beam configurations
 - Stronger J/ψ suppression at forward compared to backward rapidity
 - $\psi(2S)$ suppression independent of beam configurations
 - Good description by models (except $\psi(2S)$ at backward rapidity) but with different assumptions
- Interplay of initial and final state effects



Prompt/non-prompt J/ ψ production in Pb-Pb



$$R_{AA} = \frac{d^2N_{AA}}{dp_T dy} / \frac{d^2N_{pp}}{\langle N_{coll} \rangle dp_T dy}$$



- Complementary measurement to CMS and ATLAS
- Sign of prompt J/ ψ (re)generation at central collisions
- Prompt J/ ψ R_{AA} described by models including quarkonium dissociation (regeneration) at high (low) p_T
- Similar R_{AA} values for non-prompt J/ ψ and non-prompt D^0
- Non-prompt J/ ψ R_{AA} consistent with models implementing collisional + radiative energy loss for $p_T > 5$ GeV/c

→ J/ ψ production modified by the final-state effects

The dead-cone effect in QCD

Yu. L. Dokshitzer et al. 1991 J. Phys. G: Nucl. Part. Phys. 17 1602

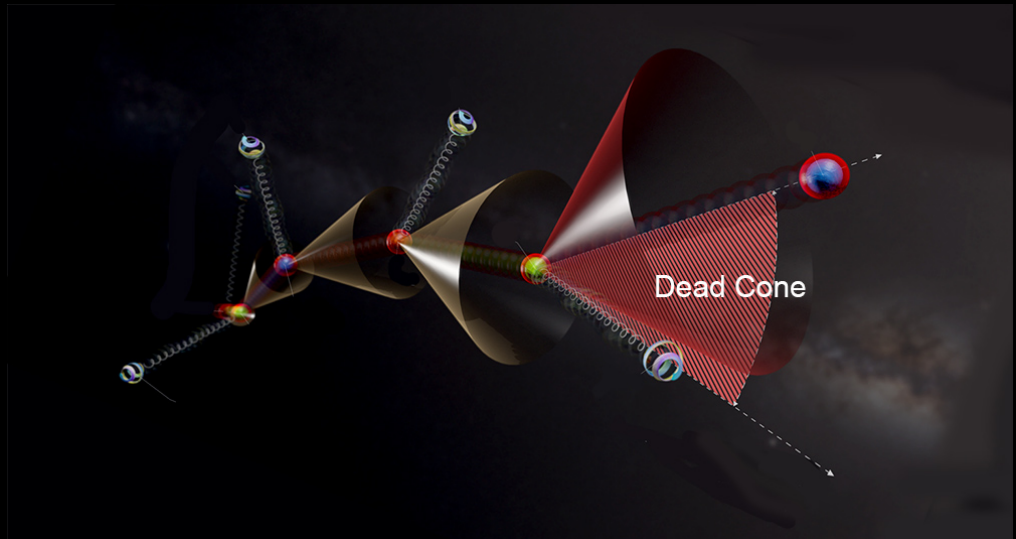
Probability of gluon radiation at small angle θ ($\theta < \theta_0 \ll 1$, $\theta_0 = m_q/E_q$)

$$\left(\frac{d\sigma}{d\omega}\right)_{q \rightarrow \bar{q}g} = \frac{\alpha_s C_F}{\pi\omega} \frac{(2\sin\theta/2)^2 d(2\sin\theta/2)^2}{[(2\sin\theta/2)^2 + \theta_0^2]^2} [1 + \mathcal{O}(\theta_0, \omega)] \sim \frac{1}{\omega} \frac{\theta^2 d\theta^2}{[\theta^2 + \theta_0^2]^2}$$

→ Gluon radiation is strongly suppressed at $\theta < \theta_0$ leading to the dead cone

First observations related to the dead cone effect:

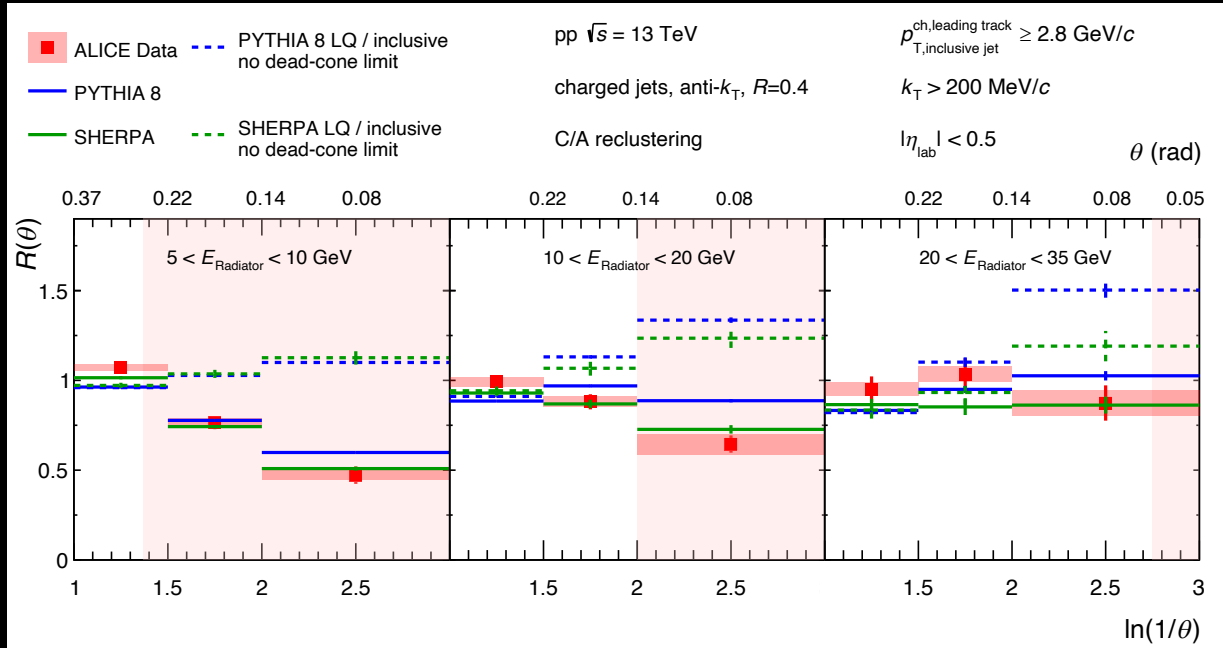
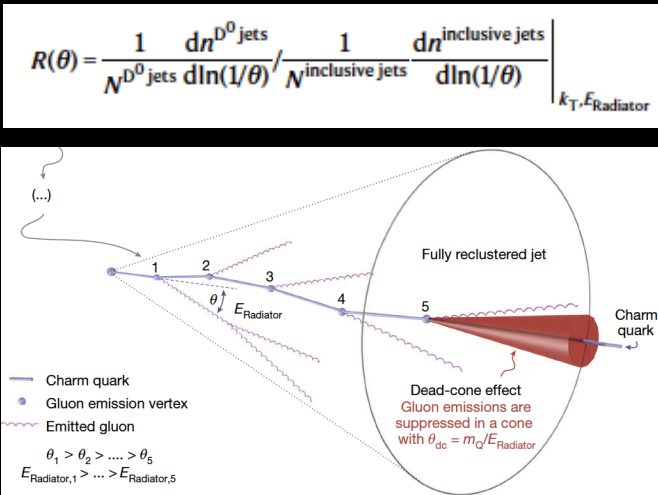
- Smaller multiplicity of e+e- events with b-jets compared to udsg-jets
DELPHI, PLB 479 (2000) 118
- Depletion in momentum density of jet constituents as a function of distance from the jet axis
ATLAS, Eur. Phys. J. C 73, 2676 (2013)



First direct dead-cone measurement → ALICE, Nature 605 (2022) 440!

Dead-cone measurement for charm quark

Nature 605 (2022) 440

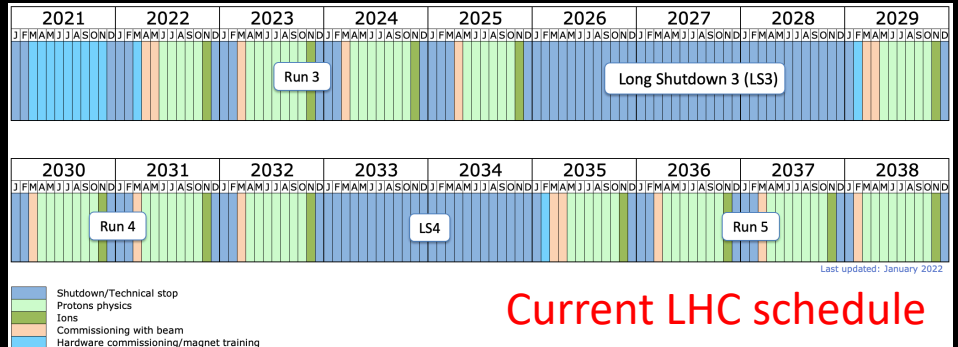


- Jets initiated by charm quark are tagged with fully reconstructed D^0 meson amongst their constituents
- Jet declustering tools allow for the sequential reconstruction of the charm quark shower
- Suppression increases with decreasing charm quark energy probed down to 5 GeV
- **The measured mass and energy dependence of the dead-cone effect follow parametric expectations from theory and are well described by MC generators**

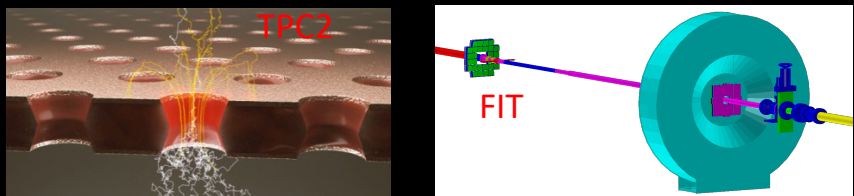
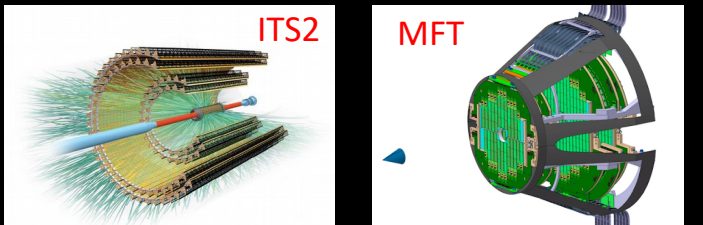
Summary

- The first measurements of multistrange baryon $p\text{-}\Xi$, $p\text{-}\Omega$ and $\Lambda\text{-}\Xi$ interactions with femtoscopy correlation techniques
 - $p\text{-}\Xi$ $p\text{-}\Omega$ strong interaction is attractive
 - No bound states seen in data
- Quarkonium production in pp, p-Pb and Pb-Pb is affected by initial and final state effects
 - Different multiplicity dependence depending on rapidity in pp collisions
 - Influence of initial state PDFs on charmonium production in p-Pb collisions
 - Final state effects dominates in Pb-Pb collisions
- The first direct dead-cone measurement for charm quarks in pp collisions
 - Mass and energy dependence of the dead-cone effect follow parametric expectations from theory and are well described by MC generators

Outlook



LS2: upgrades

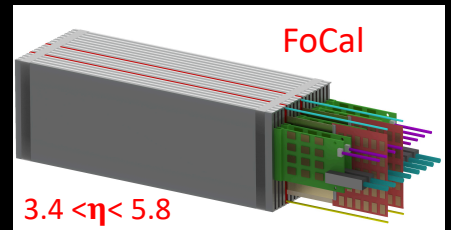


Continuous data taking

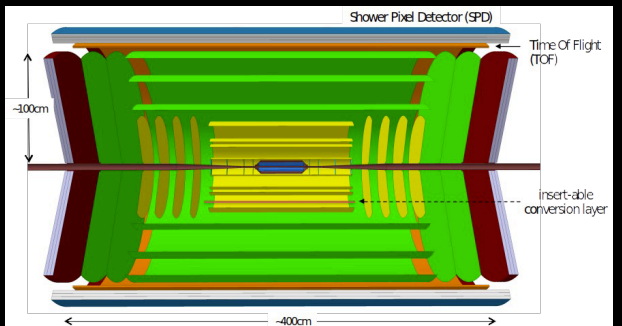
- Detector upgrade
- Online-offline computing system upgrade
- Readout electronics and trigger upgrade

10x more statistics expected!

LS3: upgrades



LS4: Future heavy-ion detector

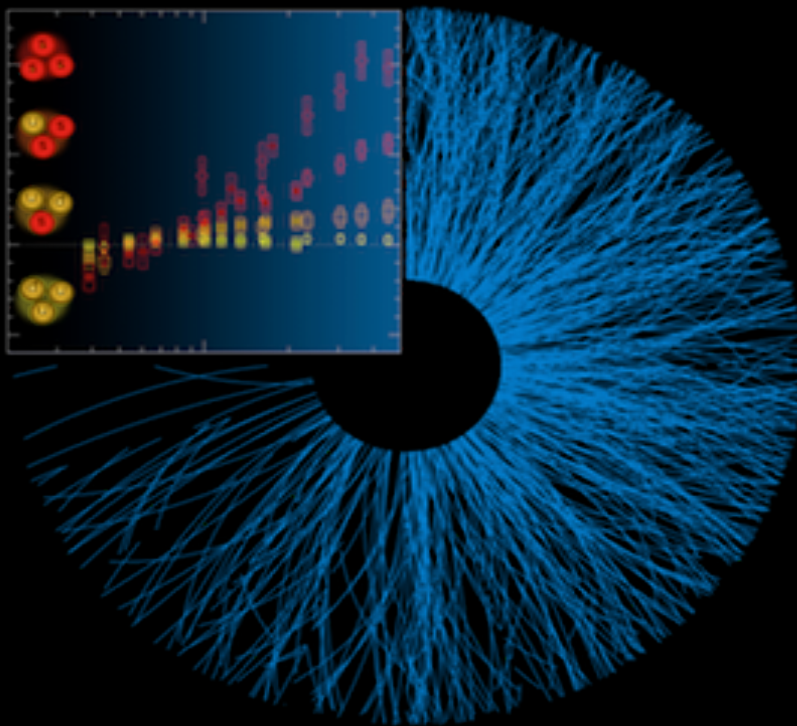


Fast Interaction Trigger (FIT)

<https://ep-news.web.cern.ch/content/new-alice-fast-interaction-trigger>



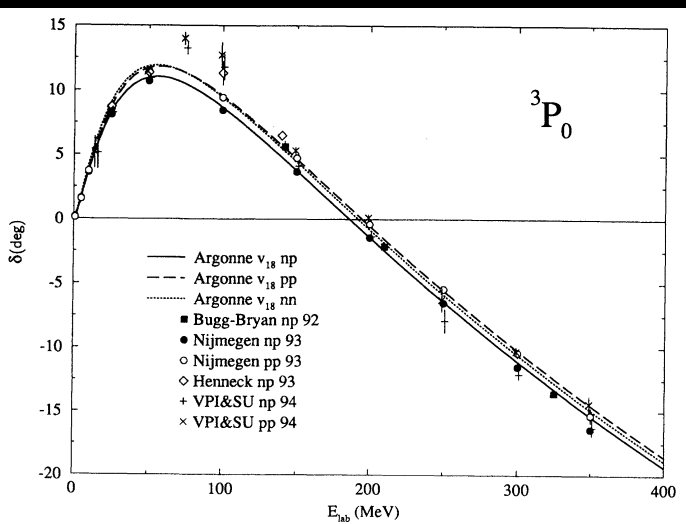
Thank you for attention!



Backup

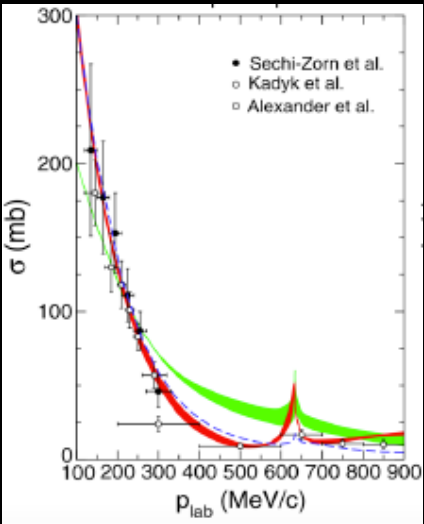
Experimental data to constrain the strong interaction

$N+N \rightarrow N+N$



R. B. Wiringa et al., PRC 51 (1995) 38

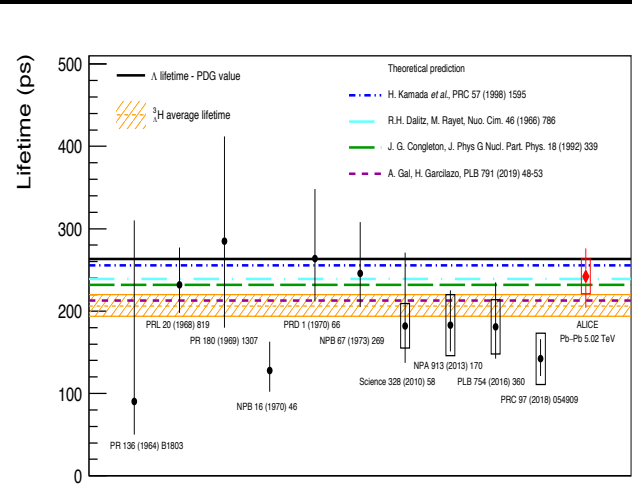
$N + \Lambda \rightarrow N + \Lambda$



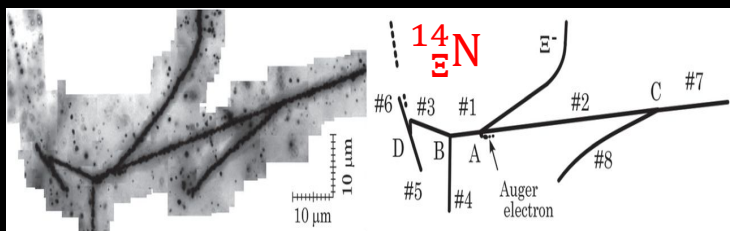
LO: H. Poinder et al. NPA 779 (2006) 244

NLO: J. Haindenbauer et al. NPA 915 (2013) 24

Hypertriton lifetime



ALICE PLB797 (2019) 134905

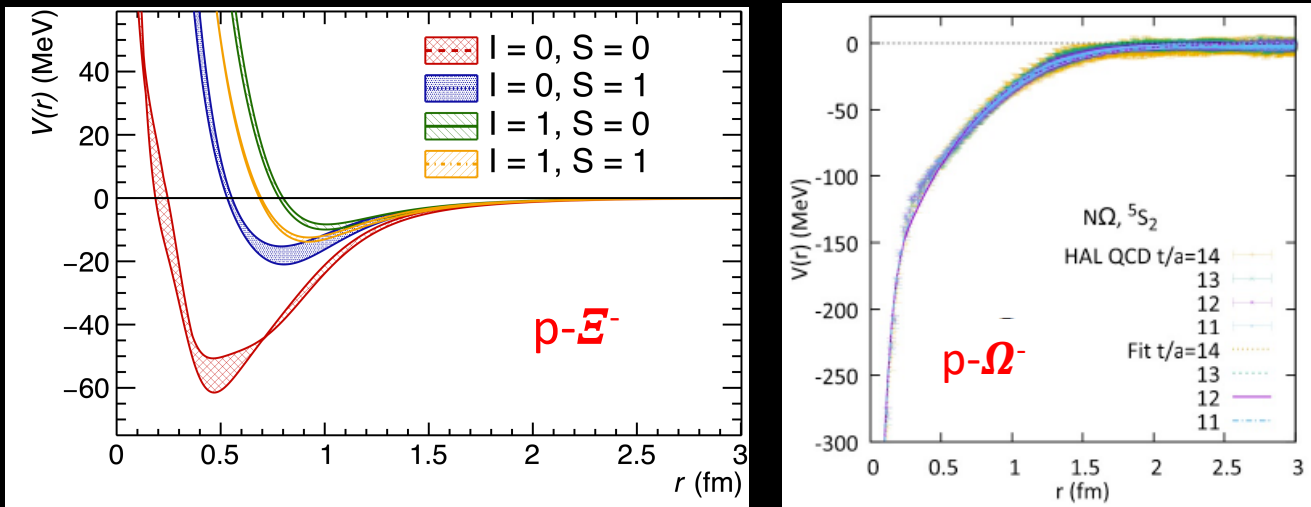
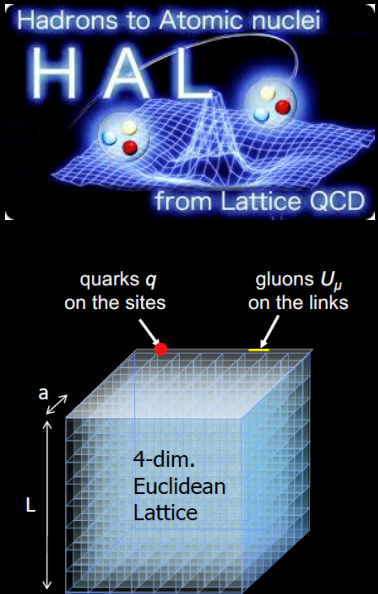


K. Nakazawa, PTEP 2015 (2015) 033D02

- Good constraints for NN interaction
- Small statistics of scattering data for hyperons
- ~1000 Λ -hypernuclei and one $^{14}\Xi N$ discovered by now

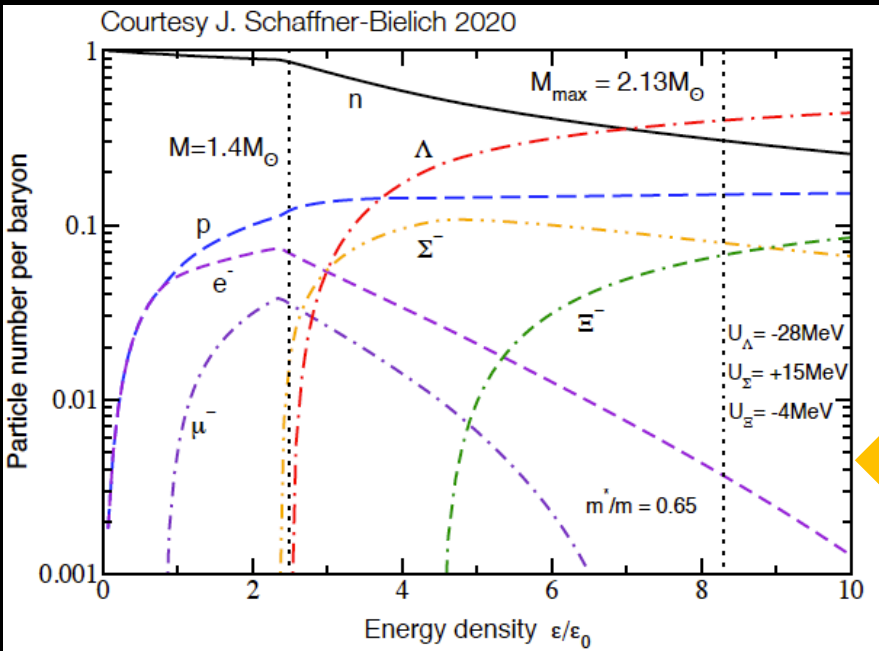
The strong interaction for p- Ξ and p- Ω on lattice

HAL QCD Coll., NPA 998 (2020) 121737, PLB 792 (2019) 284

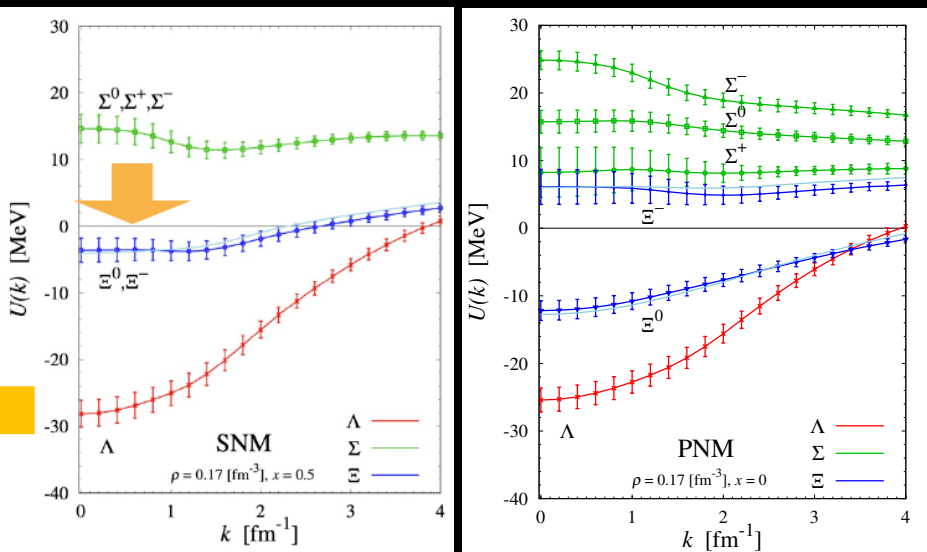


- p- Ξ interaction in four channels: isospin ($I = 0, 1$) and spin ($S=0,1$)
 - Attractive with repulsive core at small distances
- p- Ω interaction in 5S_2 ($I=1/2, S=2$) channel
 - Attractive in the whole range
 - After inclusion Coulomb interaction prediction of bound state with binding energy ~ 2.5 MeV
- p- Ω interaction in 3S_1 state does not include yet inelastic channels (e.g. $p\Omega \rightarrow \Lambda\Xi$)

Hyperon puzzle and lattice QCD



HAL QCD, T. Ioune et al. AIP Conf. Proc. 2130 (2019) 1, 020002



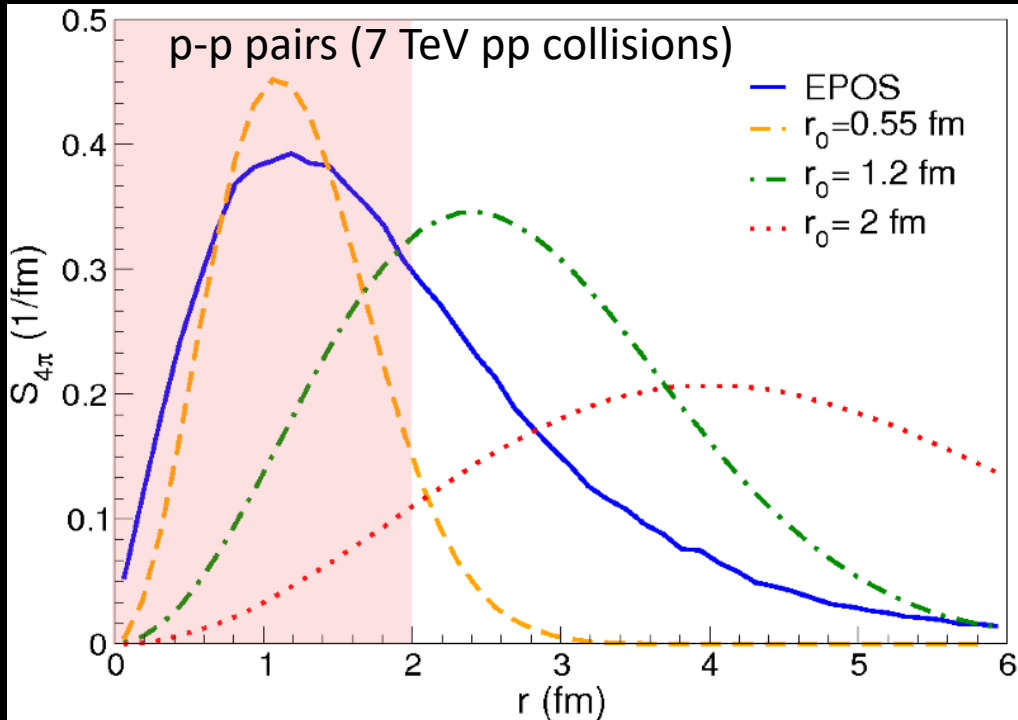
Hyperon single-particle potential

- Ξ^- attractive single-particle potential in symmetric nuclear matter (SNM) and repulsive in pure neutron matter (PNM)
- Ξ^- appears at larger densities in neutron stars

→ Resulting EoS of neutron stars is stiffer and matches astrophysical observation...

Femtoscopy in small systems

CATS, D. Mihaylov et al., Eur. Phys. J. C78 (2018) 394



Gaussian emission source:

$$S(r^*) = \frac{1}{(4\pi r_0^2)^{3/2}} \exp\left(-\frac{r^{*2}}{4r_0^2}\right)$$

Pair emission probability:

$$S_{4\pi}(r^*) = 4\pi r^2 S(r^*)$$

EPOS model predicts non-Gaussian emission source

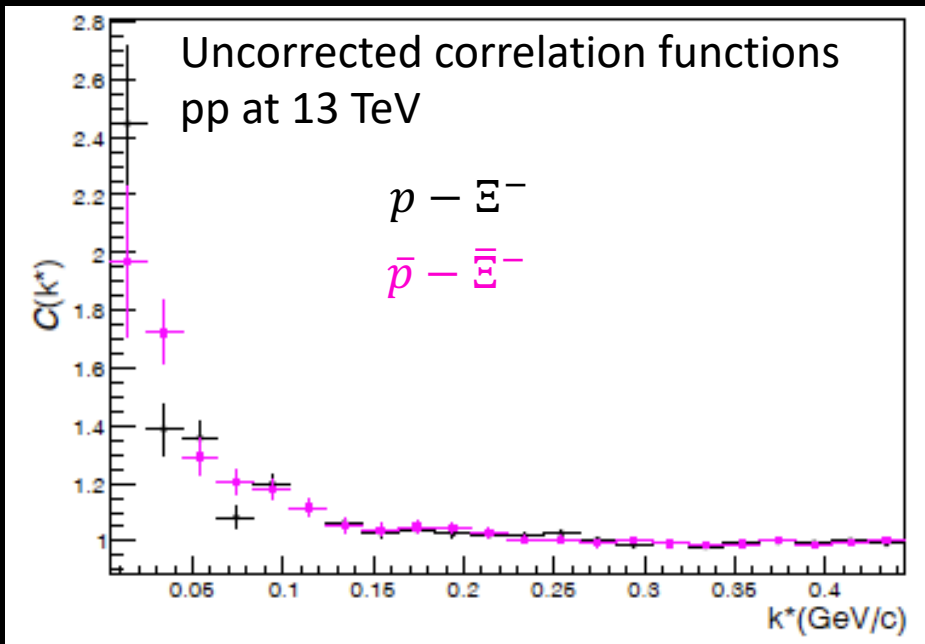
T. Pierog et al. PRC 92 (2015) 034906

- A lot of pairs is emitted from the source at distance below $\sim 2 \text{ fm}$ (typical range of strong interaction)
- Small particle emission source in pp and p-Pb collisions is essential to study the strong interaction!

Measured correlation function

Correlation function:

$$C(k^*) = \int S(r) |\psi(\vec{k}^*, \vec{r})|^2 d^3r = \zeta(k^*) \cdot \frac{N_{\text{same}}(k^*)}{N_{\text{mixed}}(k^*)}$$



Corrections $\zeta(k^*)$:

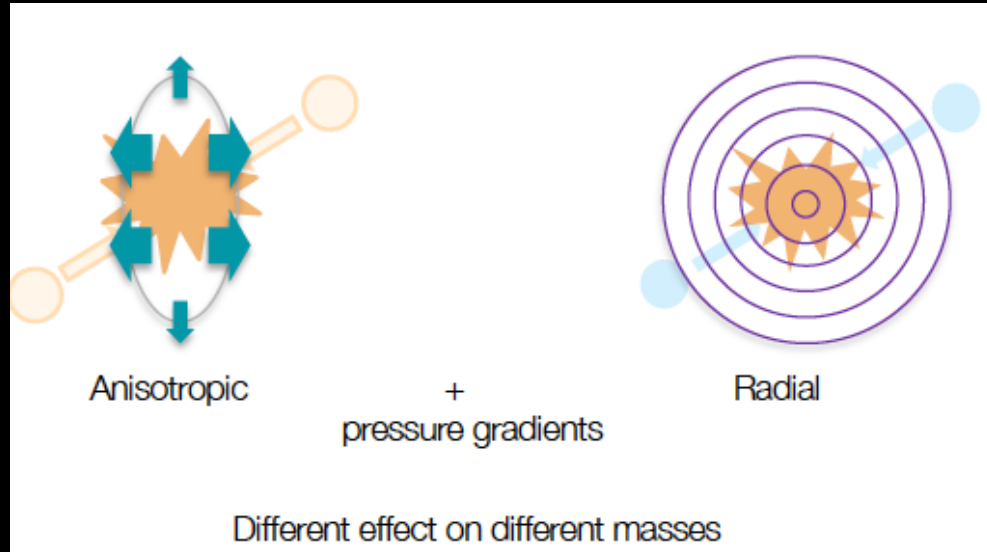
- Detector effects
- Misidentified baryons
- Proton or hyperon yields from resonances (feed-down)
- Non-femtoscopic background (energy-momentum conservation, mini-jets,...)

Feed-down to $p-\Sigma^-$

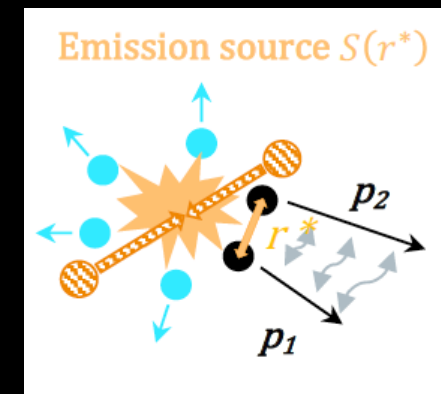
Pair	λ [%]	Pair	λ [%]	Pair	λ [%]
$p-\Sigma^-$	58.3	$p_\Lambda-\Sigma_\Omega^-$	0.08	$\bar{p}-\Sigma_{\Xi^0(1530)}^-$	0.09
$p-\Sigma_{\Xi^-(1530)}^-$	6.5	$p_{\Sigma^+}-\Sigma^-$	1.1	$\bar{p}-\Sigma_\Omega^-$	0.00
$p-\Sigma_{\Xi^0(1530)}^-$	12.9	$p_{\Sigma^+}-\Sigma_{\Xi^-(1530)}^-$	0.12	$p-\tilde{\Sigma}^-$	7.3
$p-\Sigma_\Omega^-$	0.6	$p_{\Sigma^+}-\Sigma_{\Xi^0(1530)}^-$	0.24	$p_\Lambda-\tilde{\Sigma}^-$	1.0
$p_\Lambda-\Sigma^-$	8.4	$p_{\Sigma^+}-\Sigma_\Omega^-$	0.01	$p_{\Sigma^+}-\tilde{\Sigma}^-$	0.14
$p_\Lambda-\Sigma_{\Xi^-(1530)}^-$	0.93	$\bar{p}-\Sigma^-$	0.39	$\bar{p}-\tilde{\Sigma}^-$	0.05
$p_\Lambda-\Sigma_{\Xi^0(1530)}^-$	1.87	$\bar{p}-\Sigma_{\Xi^-(1530)}^-$	0.04		

Common baryon source

Collective flow and feed-down from short lived resonances modify source size



$$m_T = \sqrt{k_T^2 + m^2}, k_T = \frac{1}{2} |p_{T1} + p_{T2}|$$



Resonances with $\text{ct} \sim r_0 \sim 1\text{fm}$ ($\Delta^{++}, N^*, \Sigma^*$)

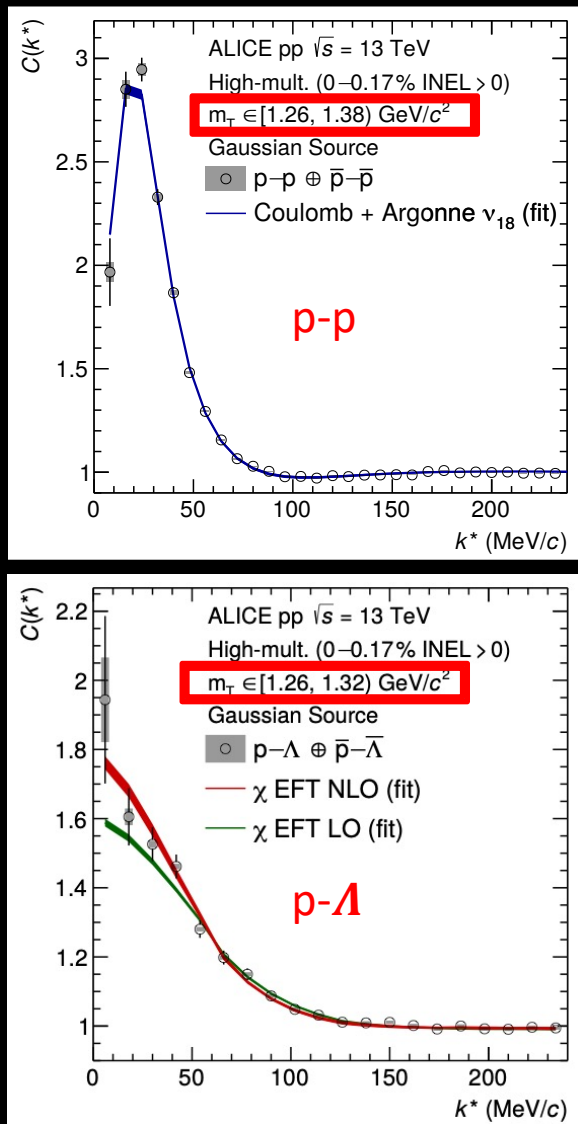
Particle	Primordial fraction	Resonances $\langle \text{ct} \rangle$
Proton	33 %	1.6 fm
Lambda	34 %	4.7 fm

U. Wiedemann U. Heinz (PRC56 R610, 1997)

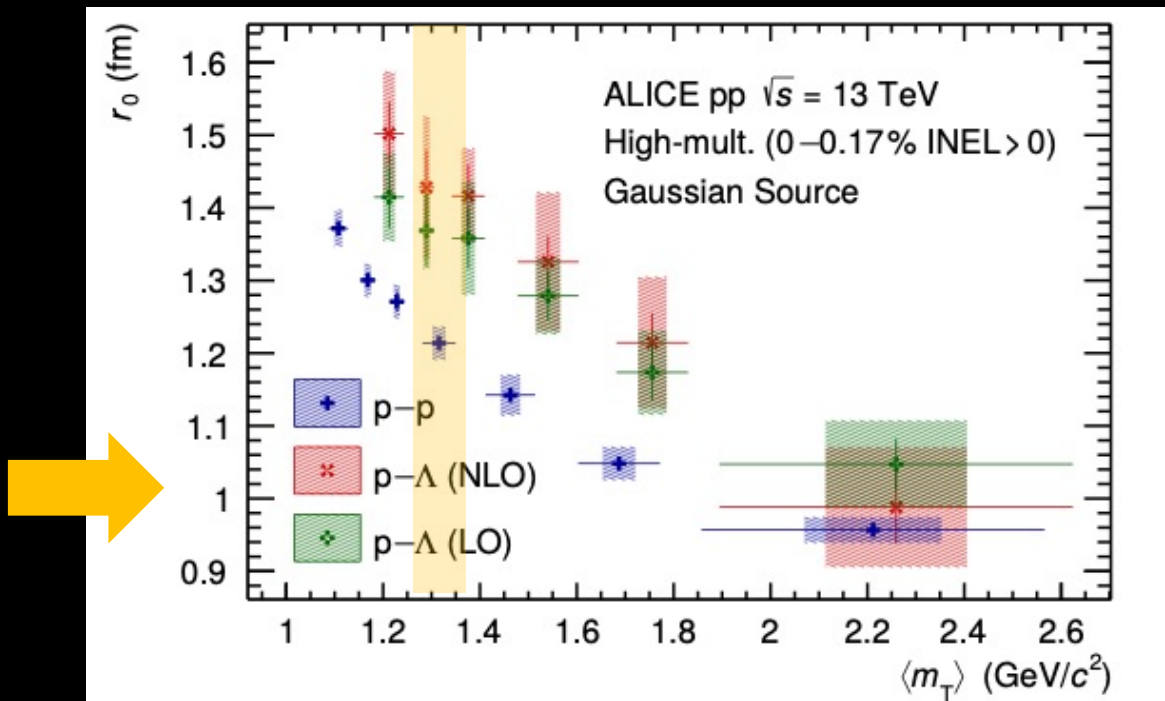
$$S(r^*) = G(r^*, r_{core}(m_T)) = \frac{1}{(4\pi r_{core}^2)^{3/2}} \exp\left(-\frac{r^{*2}}{4r_{core}^2}\right) \otimes E(r^*, M_{res}, \tau_{res}, p_{res})$$

$$E(r^*, M_{res}, \tau_{res}, p_{res}) = \frac{1}{s} \exp\left(-\frac{1}{s}\right), S = \beta \gamma \tau_{res} = \frac{p_{res}}{M_{res}} \tau_{res}$$

Common baryon source



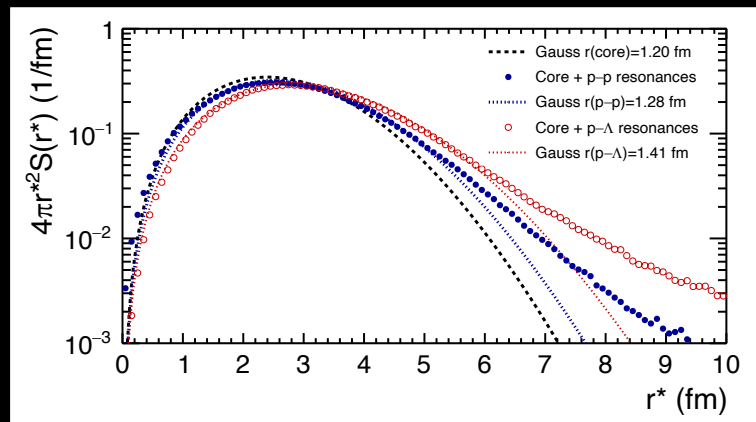
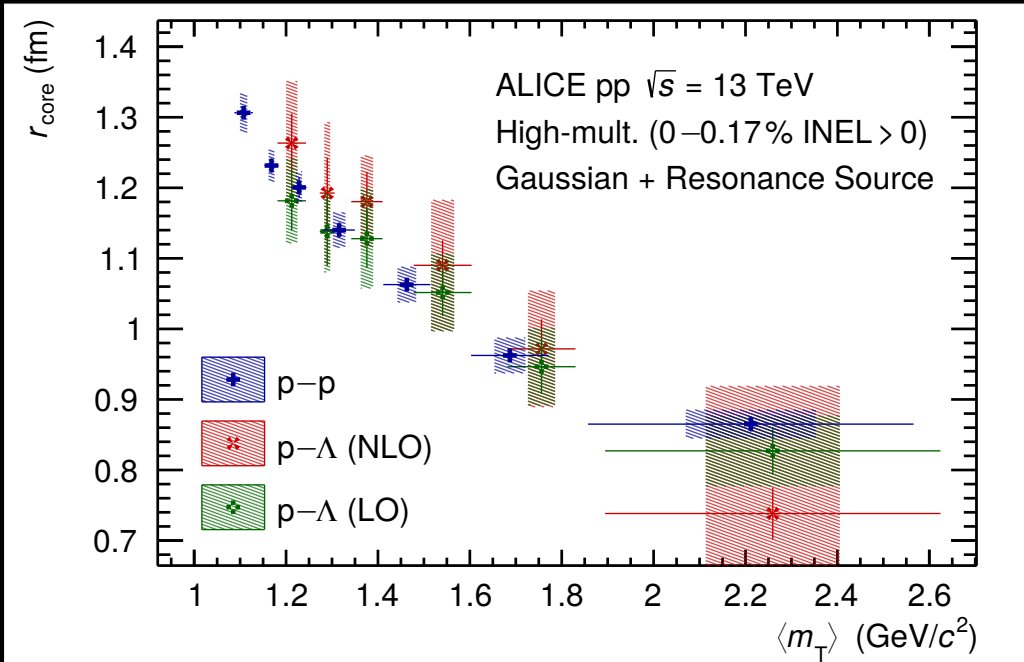
ALICE PLB 811 (2020) 135849



- Different source size depending on the baryon pair
- Gaussian source scales with m_T

Common baryon source

ALICE PLB 811 (2020) 135849



- Relative particle abundances from Statistical Hadronization Model *
- Kinematic distributions from EPOS **

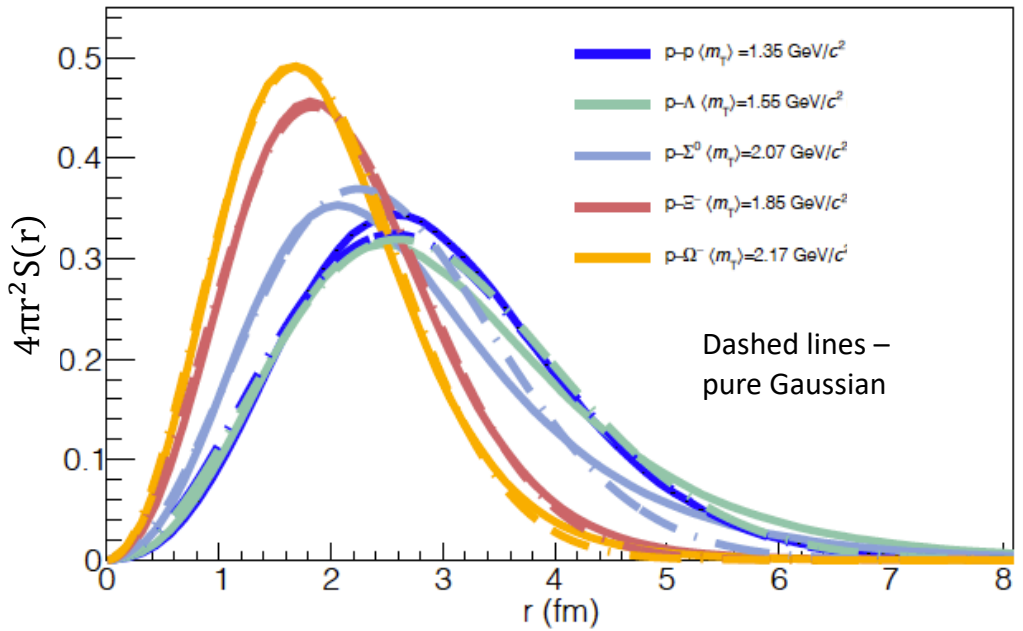
- All baryon pairs with included resonances show common m_T scaling
 → Indication of common baryon source
 → One can use p-p correlation to fix source size for other baryon pairs

* F. Becattini et al. J. Phys. G: Nucl. Part. Phys. **38** 025002

** T. Pierog et al. PRC 92 (2015) 034906

Common baryon source

Source using a Gaussian core plus resonances

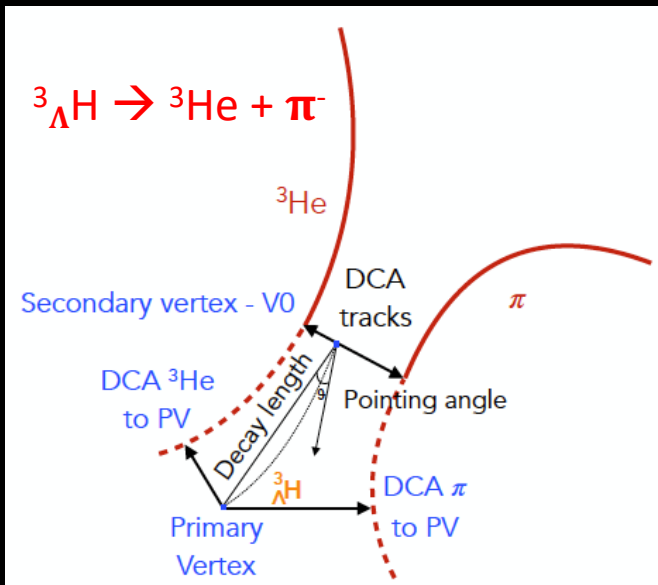


Pair	r_{Core} [fm]	r_{Eff} [fm]
p-p	1.1	1.2
p- Λ	1.0	1.3
p- Σ^0	0.87	1.02
p- Ξ^-	0.93	1.02
p- Ω^-	0.86	0.95

- Emission source for heavier pairs using p-p correlation function plus resonances
- Gaussian source with $r_{\text{eff}} = 1.02 \pm 0.05$ (0.95 ± 0.06) fm used for the p- Ξ (p- Ω) emission

(Anti-)hypertriton lifetime

arXiv:2209.07360



$$c \cdot \tau = M \cdot L \cdot c/p$$

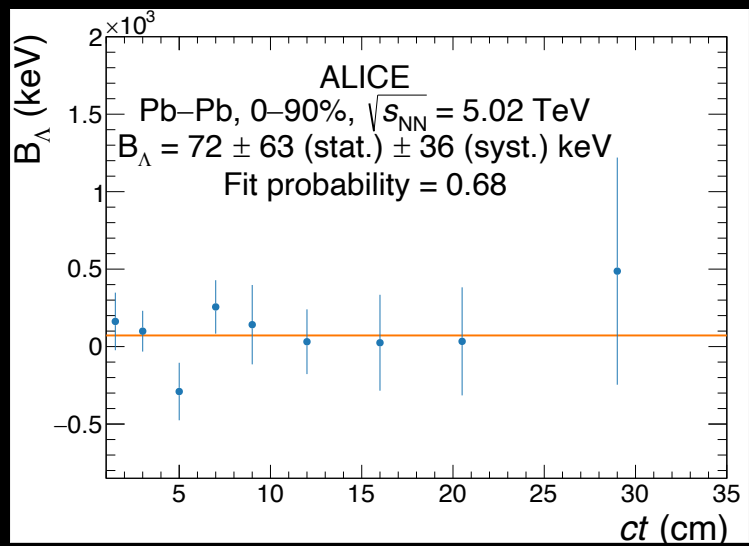
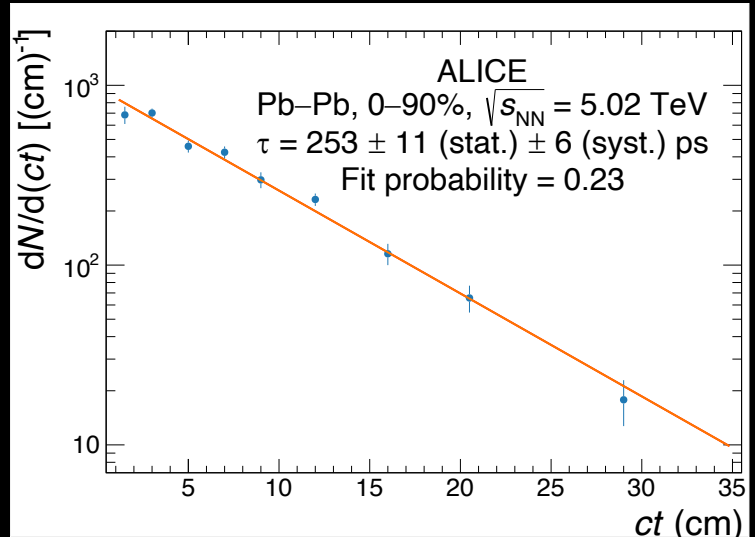
$$M = 2.99116 \pm 0.00005 \text{ GeV}/c^2$$

L - decay length

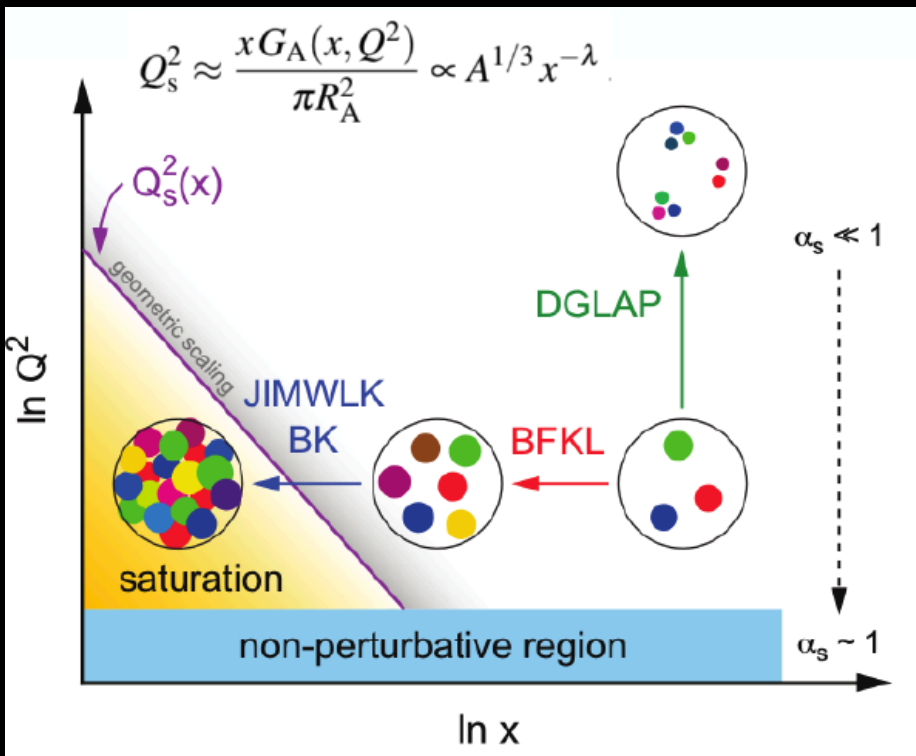
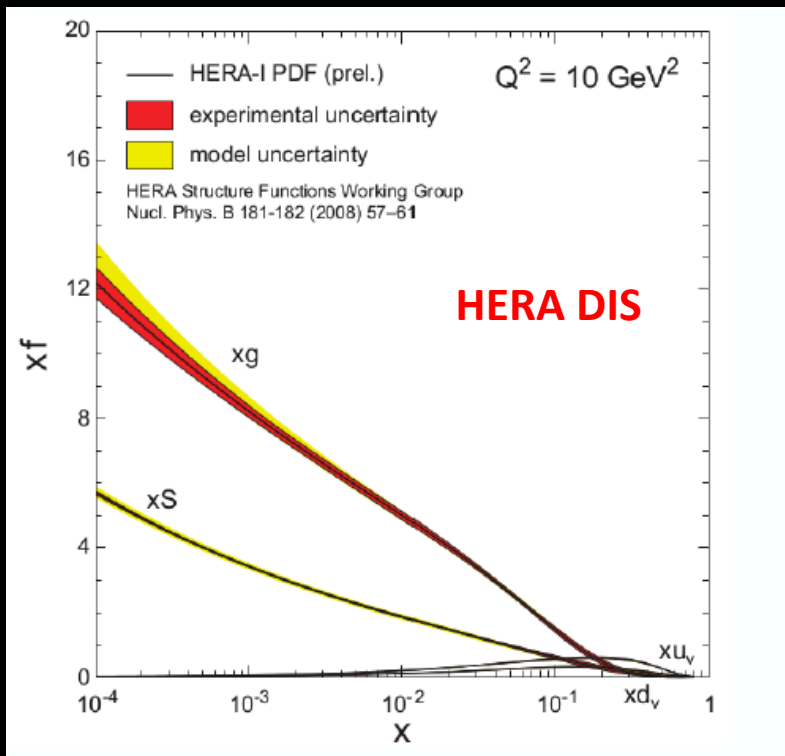
p - hypertriton momentum

Mass calculated with

$$B_\Lambda = 0.13 \pm 0.05 \text{ MeV}$$



Partonic matter



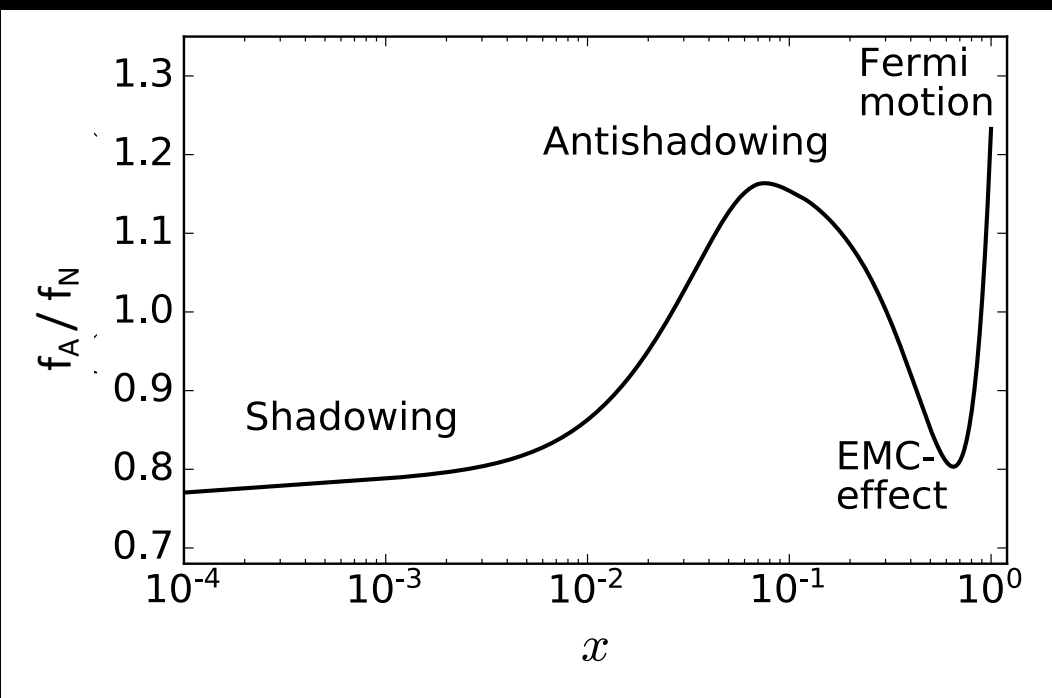
- Rise of gluon density due to gluon splitting (linear QCD evolution)
- The rise at small Bjorken-x might be tamed by gluon recombination (non-linear QCD evolution) → leading to gluon saturation at saturation scale Q_s
- The saturated gluon matter might form the Color-Glass Condensate (the universal state of matter at high energy) E. Iancu et al. Nucl. Phys.A692 (2001) 583

Nuclear PDFs

Nuclear modification of PDFs observed for the first time by EMC Coll. in μ -d (A) collisions
 J.J. Aubert et al. Phys. Lett B123 (1983)275

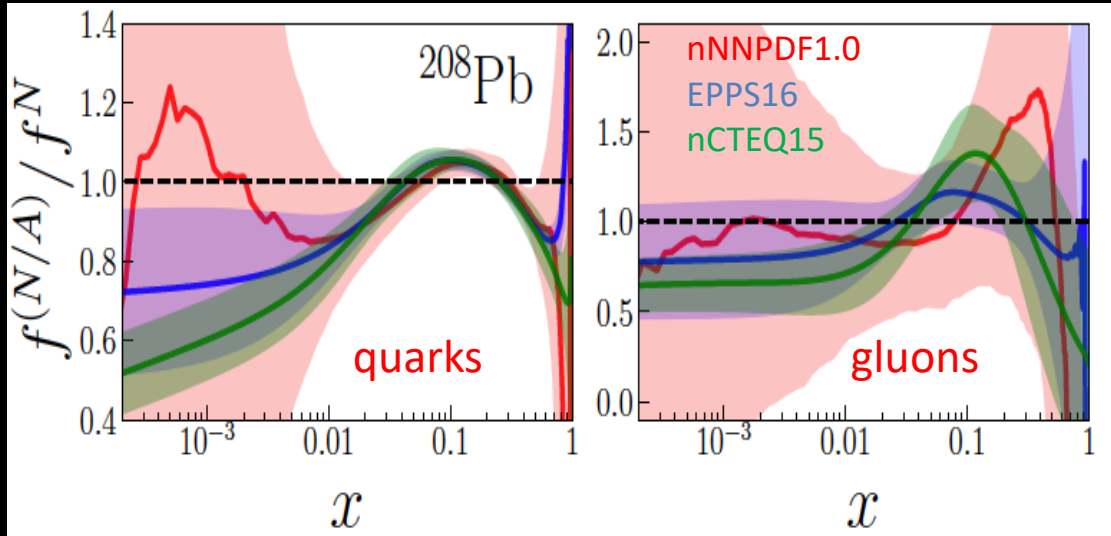
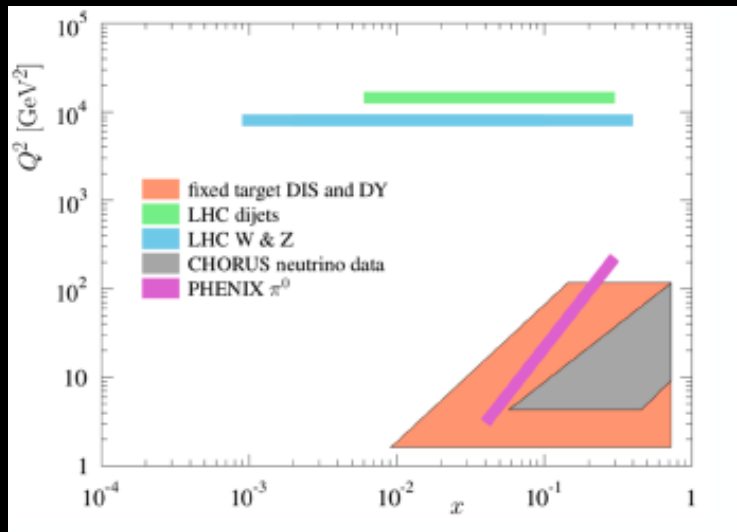
Nuclear PDFs (nPDFs):

- $f_A = R \cdot f_N$
- EMC effect is not explained yet
- Shadowing is often related to gluon saturation



Nuclear PDFs

A. Khalek et al. Eur. Phys. J. C 79 (2019) 035201

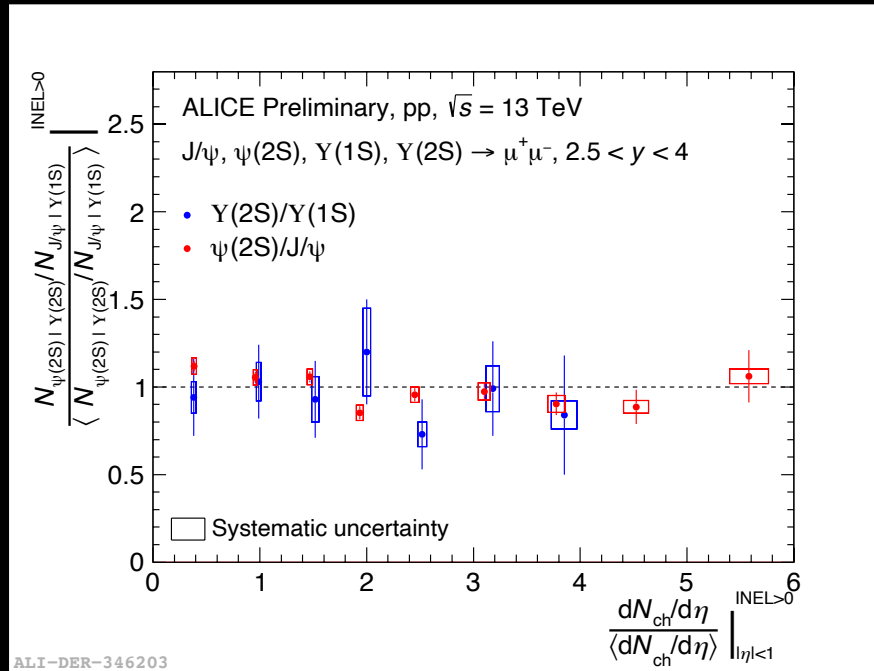
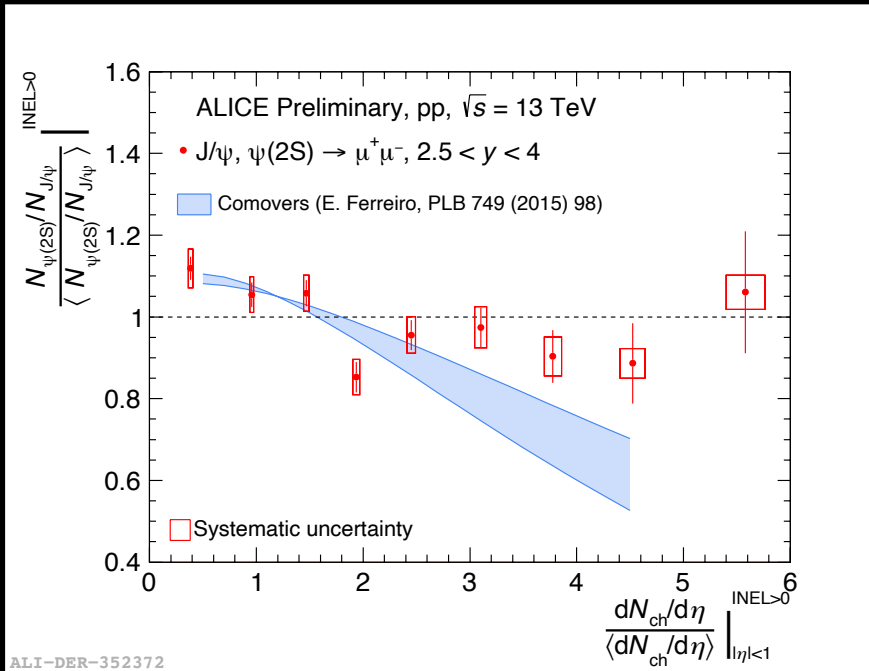


- Only few DIS measurements available ($x < 10^{-2}$)
- EPPS16 and nCTEQ15 use hadron data and functional form parametrized at small- x
- nNNPDF1.0 use only DIS data
- Large uncertainties on nuclear PDFs at small x
- Low- x accessible at forward rapidity at the LHC ($x \sim 10^{-5}$)

Exited quarkonium state production in pp



Testing final-state effects on particle production



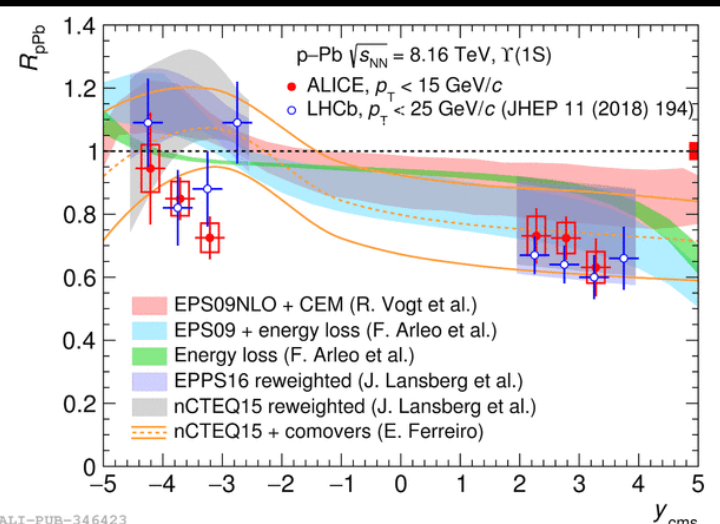
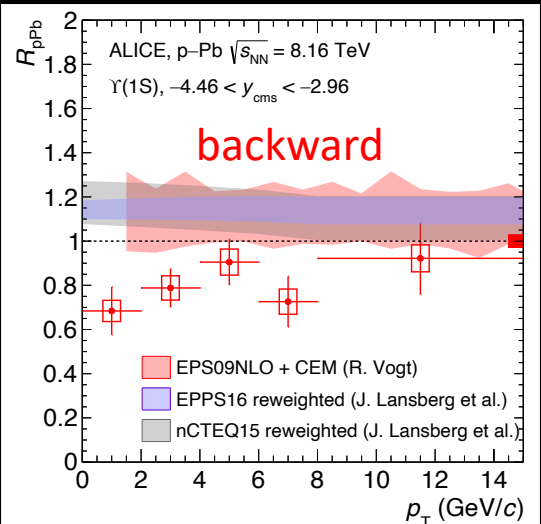
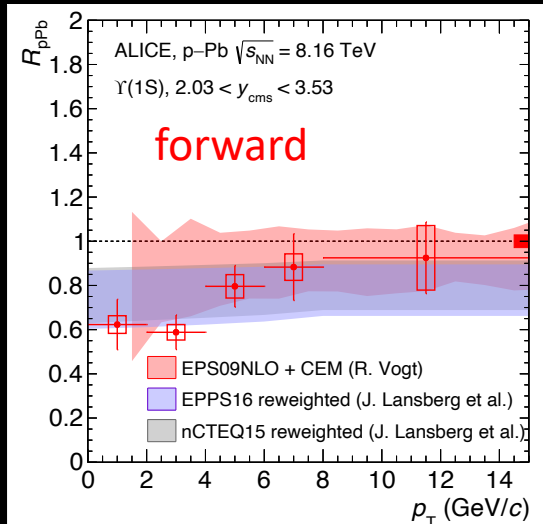
- Self-normalized $\psi(2S)/J/\psi$ ratio consistent with unity
- Comovers approach (charmonium interaction with comovers in the final state) predicts $\psi(2S)$ suppression at high multiplicity
- $\psi(2S)/J/\psi$ and $Y(2S)/Y(1S)$ ratios agree within statistical and systematic uncertainties

Bottomonium Y(1S) production in p-Pb



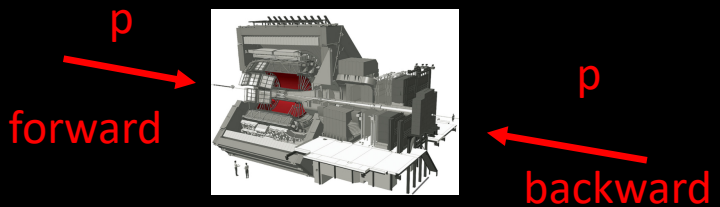
$$R_{pPb} = \frac{d^2\sigma_{pPb}}{dp_T dy} / \frac{d^2\sigma_{pp}}{A dp_T dy}$$

Phys. Lett. B 806 (2020) 135486



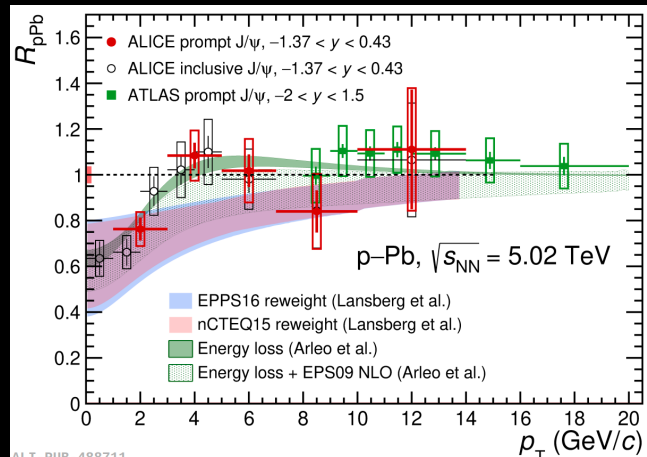
- Measurements for p-Pb (forward rapidity) and Pb-p (backward rapidity) beam configurations
- Good description by models (except at backward rapidity) but with different assumptions

→ Interplay of initial and final state effects

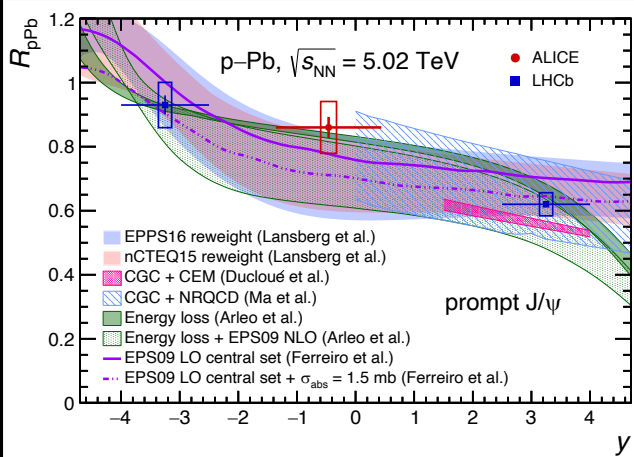


Prompt/Non-prompt J/ ψ production in p-Pb

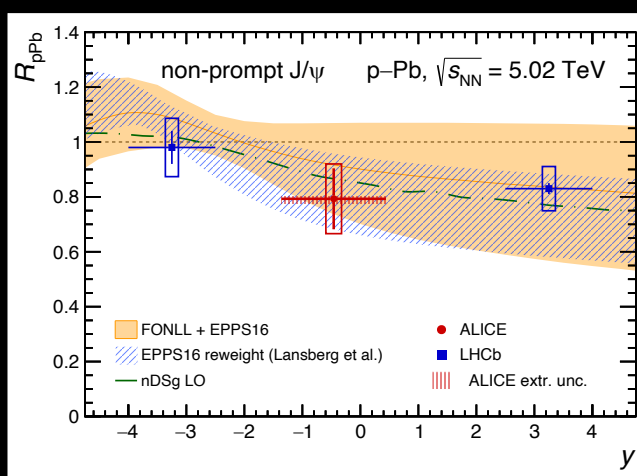
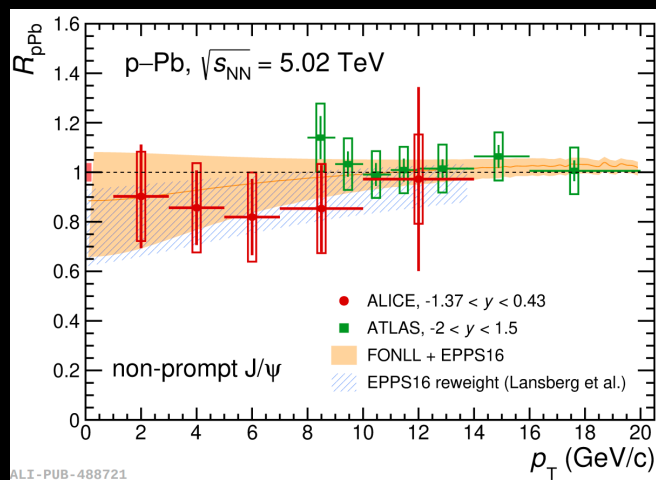
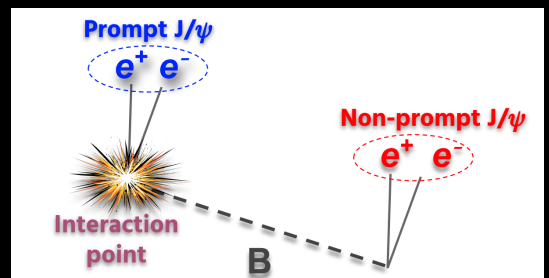
JHEP06(2022)011



ALICE-PUB-488711

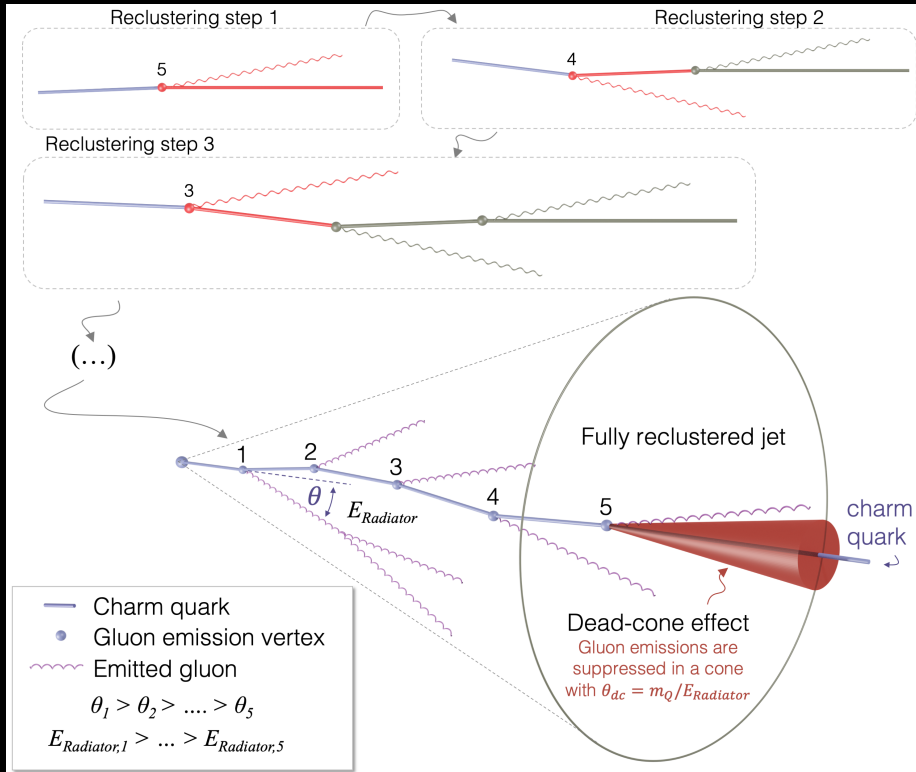


$$R_{pPb} = \frac{d^2\sigma_{pPb}}{dp_T dy} / \frac{d^2\sigma_{pp}}{A dp_T dy}$$



Dead-cone measurement for charm quark

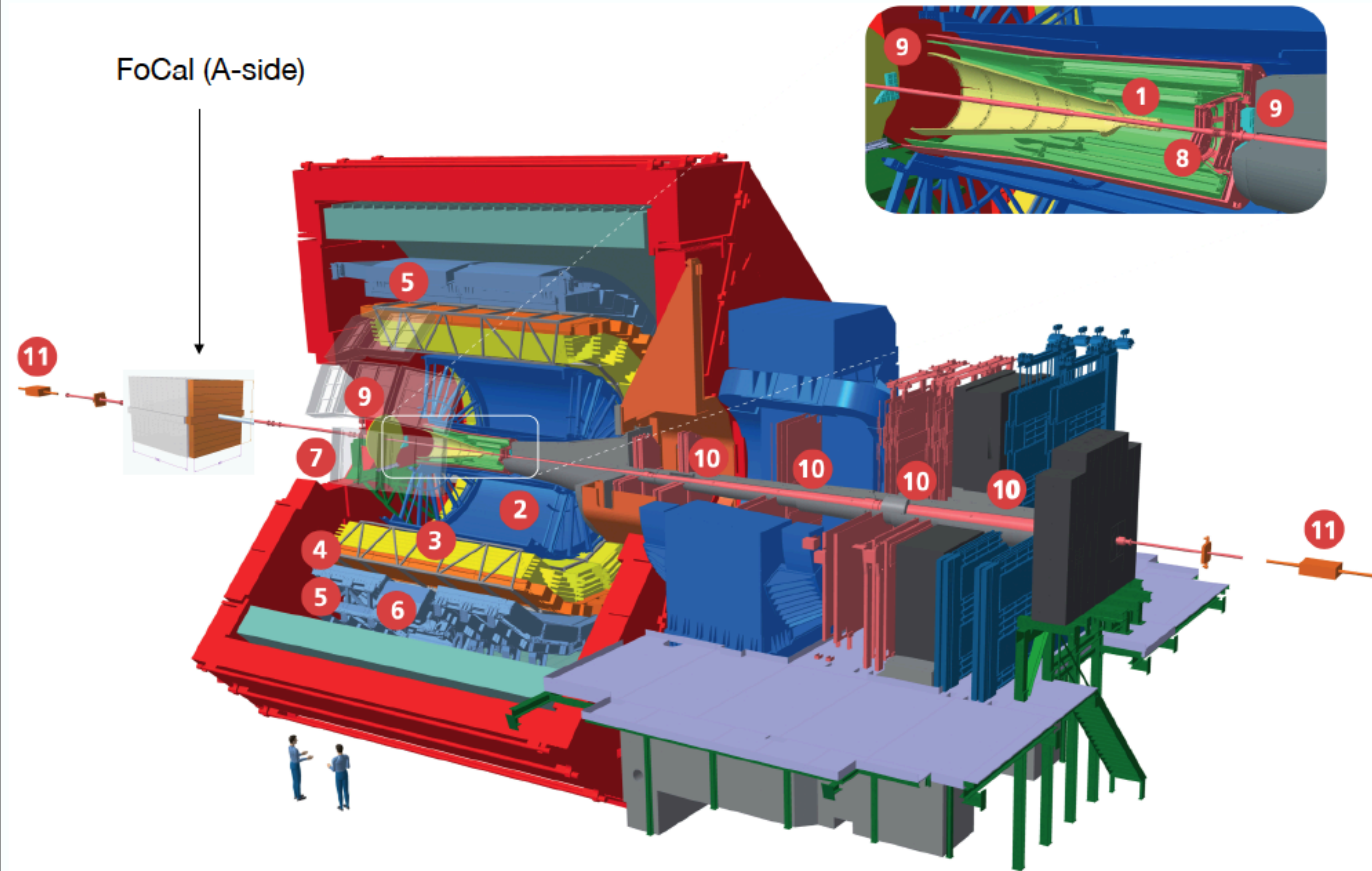
Nature 605 (2022) 440



- Jets initiated by a scattered charm quark are tagged via the presence of a fully reconstructed D0 meson amongst their constituents.
- Jet declustering tools allow for the sequential reconstruction of the charm quark shower

ALICE upgraded setup

FoCal (A-side)

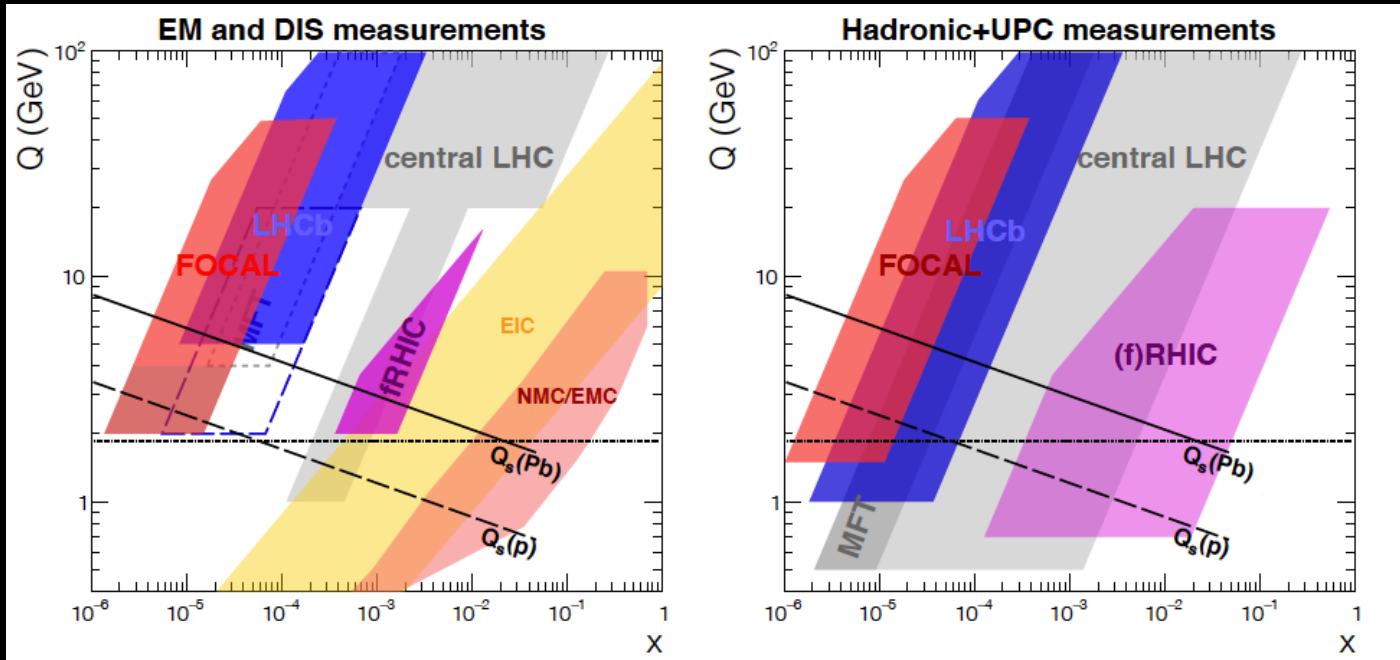


- 1 **ITS** | Inner Tracking System
- 2 **TPC** | Time Projection Chamber
- 3 **TRD** | Transition Radiation Detector
- 4 **TOF** | Time Of Flight
- 5 **EMCal** | Electromagnetic Calorimeter
- 6 **PHOS / CPV** | Photon Spectrometer
- 7 **HMPID** | High Momentum Particle Identification Detector
- 8 **MFT** | Muon Forward Tracker
- 9 **FIT** | Fast Interaction Trigger
- 10 **Muon Spectrometer**
- 11 **ZDC** | Zero Degree Calorimeter

- FIT: trigger, selection of high multiplicity and UPC collisions,...
- MFT: prompt/non-prompt charmonia, low-mass Drell-Yan,... ($2.5 < \eta < 4.0$)
- FoCal (Run4): neutral mesons, isolated photons, jets, ... ($3.4 < \eta < 5.8$)

FoCal and low-x measurements at LHC

ALICE-PUBLIC-2019-005



Explore non-linear QCD evolution at small- x to constrain nuclear PDFs (gluon saturation?)

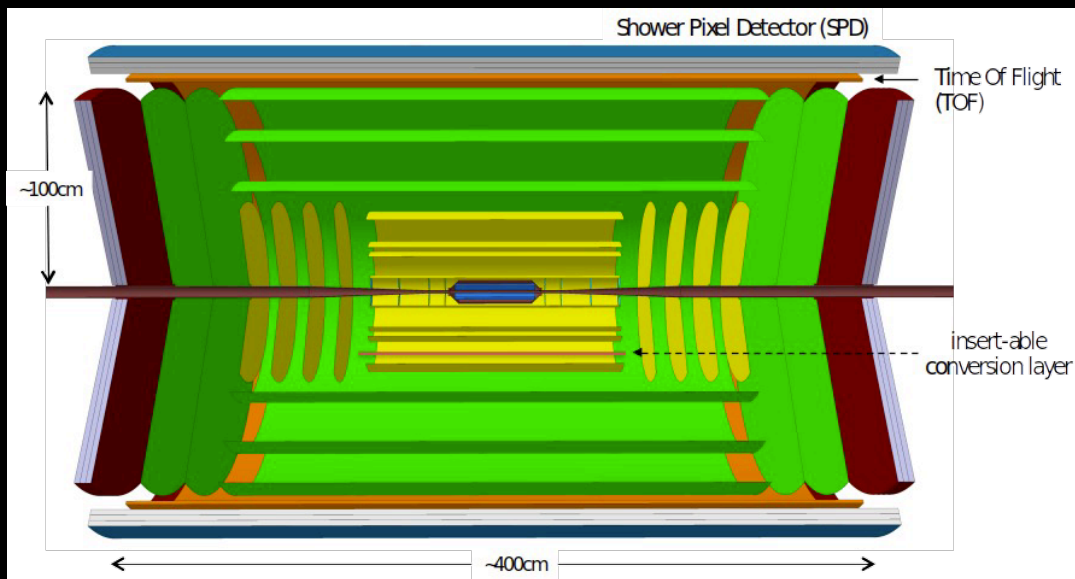
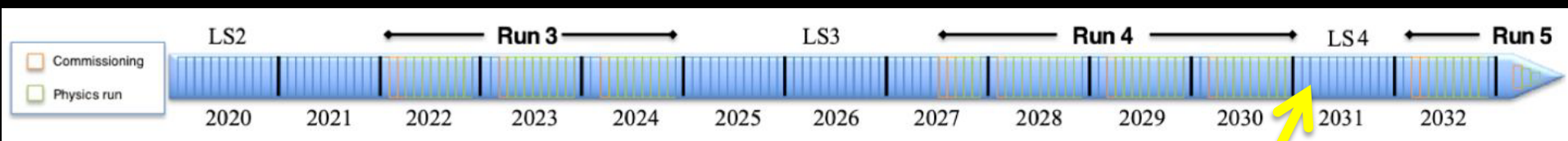
Rich low- x experimental program at LHC

- Measurements of isolated- γ , DY, open charm and UPC
- Test factorization/universality
- Complementary to fRHIC and EIC

Future Heavy Ion Detector

Possibility to extend heavy ion measurements at the LHC beyond 2030

arXiv:1902.01211



Physics:

- Heavy flavor and quarkonia
- Low mass dielectrons
- Soft photons and hadrons
- BSM

Design guidelines:

- All silicon detector
- High rate capability: $\sim 10^{34}/\text{cm}^2/\text{s}$ ($\sim 50x$ Run3-4)
- Vertex spatial resolution: $\sim 1 \mu\text{m}$
- Tracking over wide kinematic range
 - $30 \text{ MeV}/c < p_T < 10 \text{ GeV}/c$
 - $|\eta| < 4.0$